UNIVERSITY OF CALIFORNIA

Santa Barbara

Understanding calcium carbonate crystallization processes and the effects of saccharide surface interactions

A Thesis submitted in partial satisfaction of the requirements for the degree

Master of Science in Chemical Engineering

by

Katherine Ann Brune

Committee in charge:

Professor Bradley Chmelka, Chair

Professor Michael Doherty

Professor Baron Peters

September 2016

The thesis of Katherine Ann Brune is approved.

Baron Peters

Michael Doherty

Bradley Chmelka, Committee Chair

June 2016

ABSTRACT

Understanding and controlling carbonate crystallization processes and the effects of saccharide surface additive interactions

by

Katherine Ann Brune

Biological organisms are able to selectively synthesize and stabilize different polymorphs of calcium carbonate, including metastable vaterite and amorphous calcium carbonate (ACC), in a process known as biomineralization. Stabilization is accomplished by introducing other ions, such as magnesium or silicate, into the calcium carbonate material to stabilize the formation of less energetically favorable polymorphs, and also via interactions of biomolecules, such as proteins or saccharides, with the particle surface to slow the kinetics of the crystallization processes. In this work, the effects of two different saccharide surface additives, glucose and sucrose, on the crystallization process of amorphous calcium carbonate were investigated. The crystallization process was characterized using solid-state nuclear magnetic resonance (NMR) spectroscopy, wide-angle x-ray diffractometry (XRD), transmission and scanning electron microscopy (TEM and SEM), and nitrogen adsorption porosimetry. Both the glucose and sucrose adsorbates delayed the onset and progression of crystallization of amorphous calcium carbonate, though the respective products of the crystallization process differed. Adsorbed glucose surface favored the formation of the thermodynamically stable calcite polymorph, while adsorbed sucrose favored the formation of the metastable vaterite polymorph. The observed differences likely arose from the fact that glucose is a reducing saccharide that interacted with the surface of the amorphous calcium

carbonate particles primarily via electrostatic interactions, while sucrose, a non-reducing saccharide, interacted with the particle surfaces via hydrogen bonding in addition to electrostatic interactions. Furthermore, initial studies of adsorbed maltose (reducing saccharide) and trehalose (non-reducing saccharide) revealed that these surface additives exhibited the same inhibition of crystallization.

Table of Contents

1. Background and motivation

The study of crystallization processes is of interest due to the importance of crystallization in a variety of applications ranging from pharmaceuticals[1–3] to catalysis,[4–6] as well as its significance in biological and environmental systems.[7,8] Many applications for crystalline products rely on the ability to selectively synthesize crystals with specific characteristics or structures, and oftentimes metastable crystal structures provide interesting properties that lead to applications unlike those of the thermodynamically stable counterparts. An understanding of the thermodynamic and kinetic factors involved in the selective nucleation, growth, and stabilization of these metastable polymorphs presents a significant challenge that is relevant from both fundamental and technological perspectives.

Calcium carbonate is a key example of a material with multiple crystal structures that exhibit distinct morphologies, each of which are relevant to specific biological and technological applications. Three anhydrous crystalline polymorphs are known to exist; calcite, aragonite, and vaterite, as well as an amorphous form termed amorphous calcium carbonate (ACC). Calcite exhibits a rhombohedral morphology with a trigonal crystal system, while aragonite forms high aspect ratio needles with an orthorhombic crystal system (Figure 1a-b, e-f). Vaterite and amorphous calcium carbonate both form spherical particles (Figure 1g-h), with ACC exhibiting a lack of structural order characteristic of an amorphous material (Figure 1d). Vaterite is currently thought to have a hexagonal crystal system, however the exact structure is still widely disputed (Figure 1c).[9–11] The morphological and structural differences exhibited by the calcium carbonate polymorphs have led to varied applications that utilize these distinct characteristics. High aspect ratio aragonite crystals serve as a filler in the paper industry to increase the brightness of paper products and are

furthermore known to increase tensile strength in cements.[12,13] Both vaterite and amorphous calcium carbonate particles have potential applications in the pharmaceutical industry, and vaterite is also utilized in printing applications.[14–16] Additionally, amorphous calcium carbonate is an ideal building block from which to selectively synthesize other calcium carbonate polymorphs via a templated growth process,[17] exemplified in its use by biological organisms to form exoskeletal features.[8,18,19]

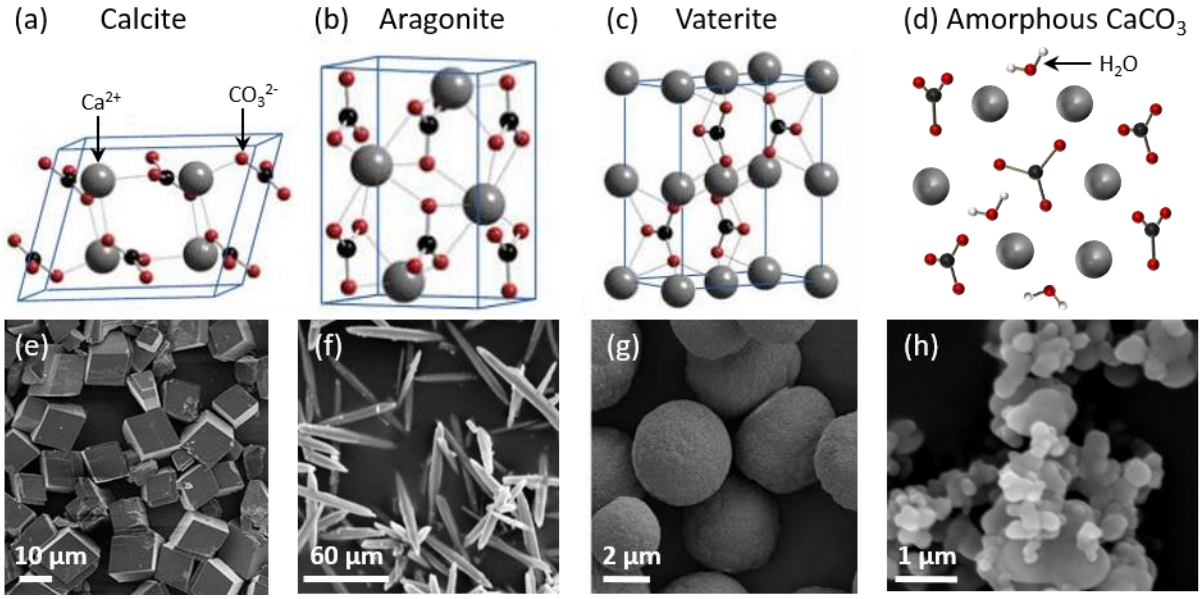

Figure 1. Unit cells of the three anhydrous calcium carbonate polymorphs (a) calcite, (b) aragonite, and (c) vaterite (reproduced from Weller et al.[20]), as well as a representation of the disordered, hydrated structure of (d) amorphous calcium carbonate (ACC). Scanning electron micrographs of synthetic (e) calcite, (f) aragonite, (g) vaterite, and (h) amorphous calcium carbonate. Calcite SEM image reproduced from Xiao et al.,[21] aragonite SEM image reproduced from Hu et al.,[22] and vaterite SEM image reproduced from Andreassen et al.[23]

Although each calcium carbonate polymorph has unique applications, several of the structures are highly metastable and therefore are difficult to synthesize and stabilize. The polymorphs range in stability from the most thermodynamically stable, calcite, to the more metastable, aragonite, vaterite, and ACC (Figure 2a). The precipitation diagram in Figure 2b shows that calcite is the most thermodynamically stable reaction product, however the other metastable polymorphs may precipitate and become kinetically stabilized under certain

solution conditions during synthesis. According to Ostwald's step rule, the most disordered metastable polymorph will initially precipitate as it is structurally most similar to the disordered nucleation clusters that form in solution and therefore is closest in free energy to the clusters.[24] Depending on the solution conditions such as pH, temperature, ionic strength, and the presence of different ions or additives, the metastable polymorphs that initially form may be stabilized instead of undergoing dissolution and reprecipitation to form more thermodynamically stable structures.

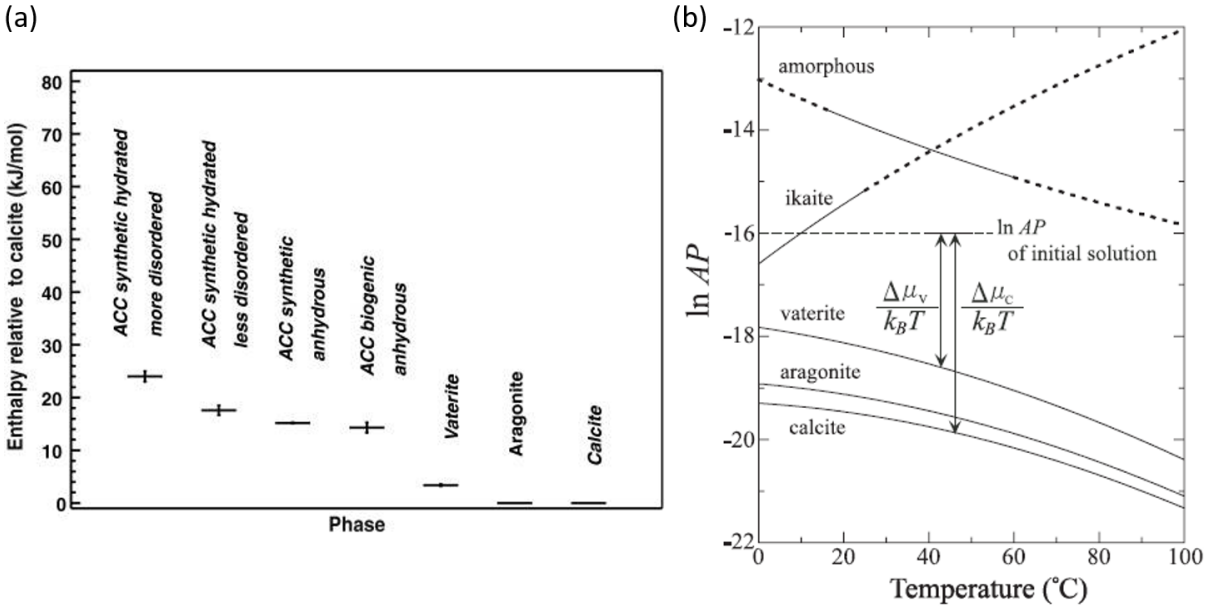

Figure 2. (a) Enthalpies of the calcium carbonate polymorphs relative to the most thermodynamically stable calcite polymorph. Reproduced from Radha et al.[25] (b) Precipitation diagram for $CaCO_3$ polymorphs showing a semi-logarithmic plot of the activity product of calcium and carbonate ions as a function of temperature. Equilibrium curves for the formation reaction of each polymorph are plotted as functions of temperature and illustrate the relative thermodynamic stability of each structure. Reproduced from Kawano et al.[26]

Despite large differences in stability, the various polymorphs of calcium carbonate are found throughout nature in geological minerals and biological organisms. While calcite, vaterite, and aragonite are the only polymorphs that occur geologically, biological organisms are able to selectively synthesize and stabilize all of the different structures in a process

known as biomineralization. Sea urchin spines are composed of calcite, and are grown and regenerated using stabilized amorphous calcium carbonate precursors (Figure 3a).[8] Abalone shells are made up of stacks of aragonite platelets (nacre) (Figure 3b) on top of a calcite shell, while lobster shells are composed of stabilized amorphous calcium carbonate (Figure 3c).[18,19] Of particular interest is the stabilization of the highly metastable amorphous calcium carbonate polymorph. Stabilization of ACC in biomineralization is thought to occur via the introduction of different additive species including ions such as magnesium, phosphates, and silicates, chitosan and chitin (biological polysaccharides), and biological proteins composed of various amino acids,[27–31] though the specific interactions and impact on local molecular environment remains relatively unexplored.

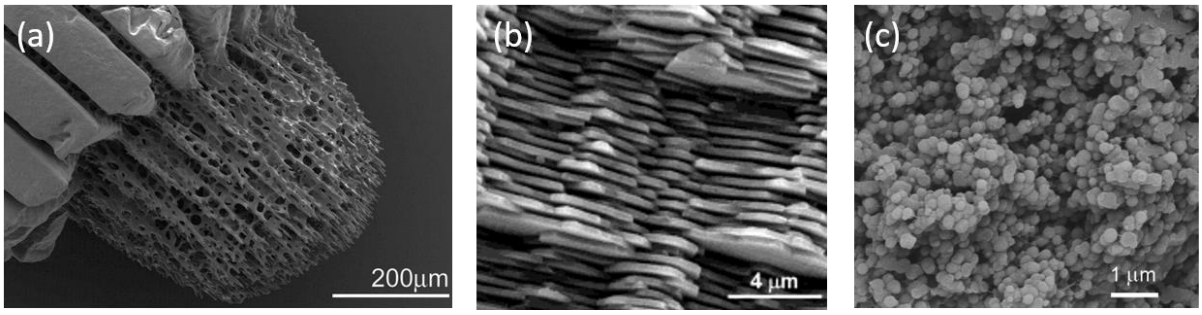

Figure 3. Scanning electron micrographs of stabilized biogenic calcium carbonate polymorphs. (a) Regenerating sea urchin spine composed of calcite, with new structure composed of amorphous calcium carbonate. Reproduced from Politi et al.[8] (b) Nacre on abalone shell made up of aragonite platelets. Reproduced from Li et al.[18] (c) Lobster exoskeleton composed of stabilized amorphous calcium carbonate. Reproduced from Reeder et al.[19]

While calcium carbonate is an interesting material from the standpoint of the industrial uses for the various polymorphs, it is also unique in that it can be synthesized from carbon dioxide, providing a consumption process to turn waste CO_2 into valuable products. Various alternative techniques exist for carbon capture and sequestration (CCS), but the main idea remains the same throughout; carbon dioxide is treated as a waste product that is sequestered in geological formations, rather than as a potential precursor to a material of value. However,

it is possible to bubble carbon dioxide through hard, alkaline brines sourced from natural underground formations or waste from mining operations and precipitate calcium carbonate. The series of reactions that occurs during this process are depicted in Figure 4. Carbon dioxide is reacted with hydroxide ions in solution, forming bicarbonate, which then reacts again with hydroxide to form carbonate ions and water. The carbonate reacts with calcium to precipitate calcium carbonate solids. Depending on factors including pH, temperature, supersaturation, and the presence of additives, any one of the calcium carbonate polymorphs may be synthesized and stabilized. The calcium carbonate formed during this process could be utilized in any manner of the industrial processes described previously or, in the case of amorphous calcium carbonate, could serve as a building block from which to synthesize other polymorphs in a templated growth process. Developing a fundamental understanding of the nucleation, growth, and stabilization of the various calcium carbonate polymorphs is necessary to design processes that can turn waste CO_2 into valuable calcium carbonate polymorphs.

$$CO_2 + OH^- \rightleftharpoons HCO_3^- \qquad \text{Eq. (1)}$$

$$HCO_3^- + OH^- \rightleftharpoons CO_3^{2-} + H_2O \qquad \text{Eq. (2)}$$

$$H_2O \rightleftharpoons OH^- + H^+ \qquad \text{Eq. (3)}$$

$$Ca^{2+} + CO_3^{2-} \rightleftharpoons CaCO_3\ (s) \qquad \text{Eq. (4)}$$

Figure 4. Mechanism by which carbon dioxide reacts with the calcium and hydroxide ions found in hard, alkaline brines to form calcium carbonate precipitates. The polymorph of calcium carbonate that is formed from these reactions is dependent on solution conditions including pH, temperature, and ion concentrations.

The overarching objective of this work is to gain insights into the crystallization process of amorphous calcium carbonate in order to better select and understand the types of additives and interactions that might stabilize the amorphous material or direct crystallization

to a polymorph of interest. Specifically, the origin and progression of crystallization in ACC are poorly understood, however developing an understanding of these processes will provide important insights into the most efficacious method for stabilization. Inspiration for the stabilization of ACC is taken from biological organisms, and the stabilized metastable ACC can be utilized as a product of value, either by direct application or by further templated crystallization to a polymorph and morphology of interest. The secondary objective following from this overarching objective is to develop a procedure wherein carbon dioxide can be utilized to produce a stabilized metastable calcium carbonate polymorph of value. This would provide an interesting alternative to traditional CCS techniques wherein carbon dioxide is treated as a waste rather than a resource for synthesizing a variety of valuable products.

Several hypotheses arise from these specific objectives, the first being that in the solid state under conditions of high relative humidity, amorphous calcium carbonate crystallization is initiated at the particle surface and progresses inward, and therefore surface additives may be used to inhibit crystallization. Additionally, different interactions of additives with the particle surface could produce different stabilization effects. Specifically, taking inspiration from the use of modified polysaccharides by biological organisms in the stabilization of amorphous calcium carbonate, it is hypothesized that mono- and disaccharides may affect the crystallization process of amorphous calcium carbonate via hydrogen bonding and electrostatic interactions with the particle surface. Depending on the stereochemistry of saccharide utilized and whether the saccharide is reducing or non-reducing, the stabilization will occur to different extents and crystallization may result in the formation of different metastable polymorphs of calcium carbonate rather than calcite. The results of these studies

will contribute to better understanding the biomineralization process by examining the role that surface additive interactions of saccharides play in stabilizing ACC. Furthermore, determining which metastable polymorphs crystallize from ACC precursors as a result of different surface additive interactions is necessary to develop a procedure for directed crystallization.

The use of saccharides as a hydration inhibiting surface additive in silicate systems has precedent in the Chmelka group.[32] It has been found that hydrogen bonding of non-reducing saccharides such as sucrose with silicate particles inhibits hydration, while reducing saccharides such as glucose are incapable of hydrogen bonding with particle surfaces and interact primarily via electrostatic interactions which do not effectively inhibit hydration. This lends support to the aforementioned hypothesis that different saccharides may have different effects on the crystallization process of amorphous calcium carbonate due to the different types of interactions present.

Furthermore, saccharides have previously been utilized to stabilize amorphous calcium carbonate by adding large quantities during the synthesis[33] rather than post synthesis as a surface additive, which could have a significant impact on the subsequent crystallization process and development of other material properties. The crystallization process of the saccharide-stabilized amorphous calcium carbonate was not investigated and the additive interactions have never been characterized. The insights gained from this work will contribute to a better understanding of the stabilizing interactions of additive species with calcium carbonate polymorphs in order to develop products of potential value from controlled crystallization and provide better understanding of natural phenomena such as biomineralization.

2. Materials and methods

2.1. Synthesis and crystallization of amorphous calcium carbonate nanoparticles

Amorphous calcium carbonate nanoparticles were prepared by mixing a solution of 0.1 M $CaCl_2$ with a solution of 0.05 M Na_2CO_3 and 0.05 M NaOH at 4°C (Figure 5). Typical solution amounts used were 30 mL and 60 mL, respectively, and the initial solution pH was 12.8. White calcium carbonate nanoparticles immediately precipitated after the salt solutions were combined, and the resulting solution (pH 12.7) and nanoparticles were stored in an ice bath (4°C) for 30 seconds before filtration with 0.45 μm Millipore Stericup filters (Figure 5). If a saccharide additive was applied to the calcium carbonate particle surfaces, it was added in the form of a 25 wt % solution after 30 seconds and the amount added to the synthesis solution was 200% by weight of the expected calcium carbonate precipitate (assuming a 100% yield). The saccharide adsorption occurred in an ice bath at 4°C for an additional 4 minutes 30 seconds and was followed by filtration using 0.45 μm Millipore Stericup filters (Figure 5). The filter with the calcium carbonate precipitate was then placed in liquid nitrogen in preparation for removal of physisorbed water via lyophilization, which was allowed to occur for 48 hours. After this process, the amorphous samples were taken off of the lyophilizer, removed from the filter paper, and ground into uniformly sized aggregates. The calcium carbonate samples were then stored in a controlled humidity environment (76% relative humidity as regulated by a saturated NaCl solution) at 20°C and the crystallization process was monitored at the designated time points. For the purpose of NMR experiments, ^{13}C enriched Na_2CO_3 was used to prepare the calcium carbonate nanoparticles to expedite measurements.

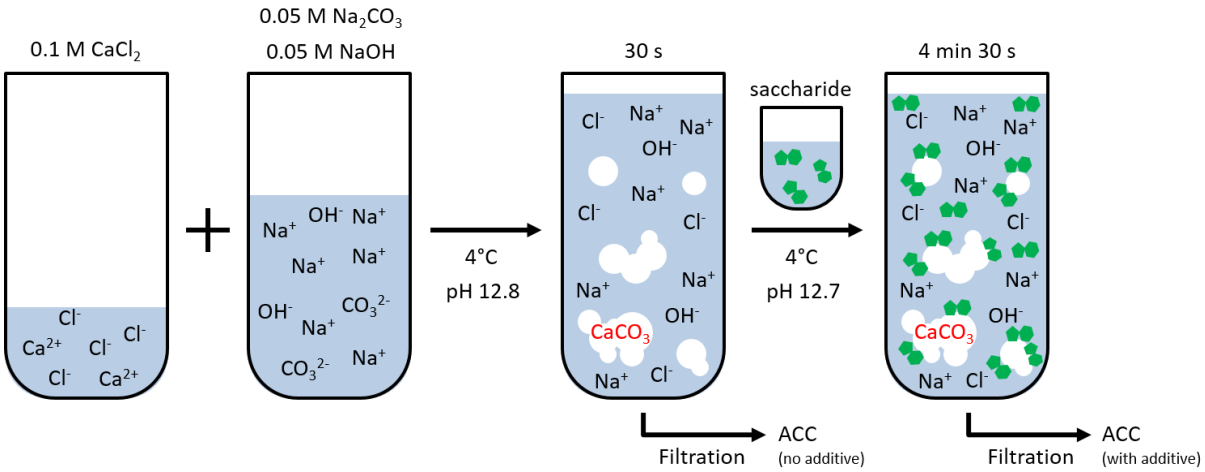

Figure 5. Schematic diagram depicting the formation of amorphous calcium carbonate nanoparticles at 4°C, pH 12.8 without and with saccharide additives.

2.2. Methods

2.2.1. Nuclear magnetic resonance (NMR) spectroscopy

Nuclear magnetic resonance (NMR) spectroscopy is a solution- and solid-state technique sensitive to local atomic order (<1 nm). Samples are placed into a magnetic field and radio frequency (RF) pulses are applied to polarize the NMR active nuclear isotopes, inducing Larmor precession at a frequency that is indicative of the extent of electronic shielding of the nuclei, which in turn provides information regarding local molecular environments and interactions. Different RF pulse sequences may be applied to the magnetized nuclei in order to characterize distinct properties, however the resulting signal intensity is affected significantly by the relative natural abundances and gyromagnetic ratios of the isotopes.

Solid-state single-pulse NMR experiments employ direct polarization of the nuclei of interest and provide information regarding the extents of order and relative populations of the different atomic environments present in the sample. In contrast, cross-polarization (CP) experiments employ polarization transfer to selectively detect dipole-dipole coupled heteronuclei. The signal intensity in the cross polarization experiments is therefore based

upon the molecular distance between the nuclei from which polarization is transferred and the nuclei that are detected, in addition to the quantity of the isotopes that are adjacent to each other. The same principles for the one-dimensional experiments mentioned may be extended to two-dimensional experiments, which are performed to assess intermolecular interactions between distinct atomic sites.

2.2.2. Transmission electron microscopy (TEM)

Transmission electron microscopy (TEM) images are produced by the detection of electrons that are transmitted through a sample. Based on the interactions of the electrons with the sample, information regarding morphology, density, and crystallinity can be obtained from elastic scattering and information regarding composition may be obtained from inelastic scattering and emission of x-rays. Several different modes of operation result from the detection of different categories of transmitted electrons - bright-field TEM utilizes the unscattered electrons that are passed through the sample and contrast is generated from occlusion and absorption, while dark-field TEM utilizes electrons that are deflected by Bragg scattering and contrast is generated from diffraction. Amongst other things, TEM is commonly used to characterize morphology (bright-field TEM), crystal structure and orientation (selected area electron diffraction and dark-field TEM), crystal lattice structures (high-resolution TEM), and chemical composition (electron energy loss spectroscopy, energy-dispersive x-ray spectroscopy).

2.2.3. Scanning electron microscopy (SEM)

Scanning electron microscopy (SEM) utilizes a focused beam of electrons to produce images from the detection of electrons that are emitted or backscattered from a sample surface. As the electron beam is rastered across the sample, the electrons either penetrate the

sample surface and eject electrons from the sample through inelastic scattering (secondary electrons) or are deflected from the sample surface via elastic scattering (backscattered electrons). The detection of these electrons provides information regarding morphology and structural features, while the detection of the x-rays emitted by the sample during the inelastic scattering process provides information regarding chemical composition (EDS).

2.2.4. X-ray diffractometry (XRD)

X-ray diffraction (XRD) patterns are produced by applying a beam of x-rays to a sample and detecting the x-rays that are diffracted by the sample. The resulting diffraction angles and intensities are affected by the interactions between the incident beam of x-rays and the electronic environments surrounding the nuclei in the sample, allowing for determination of the spatial distribution of the atoms in the sample. This is accomplished by applying Bragg's Law, which relates interplanar lattice spacings to the angles at which diffraction intensity is present, thus providing information regarding unit cell dimensions and crystal structures in the sample for areas of long range order (>10 nm). Furthermore, the line broadening of the reflections in the diffraction pattern may be related to the distribution of crystallite sizes present in the sample using the Scherrer equation, and the relative populations of the crystallites may be calculated from the shapes and intensities of the reflections and using Rietveld refinement.

3. Results and discussion

3.1. Crystallization of neat amorphous calcium carbonate

To determine the effects of saccharide adsorbates on the crystallization process of amorphous calcium carbonate, complete characterization of the crystallization of neat ACC was first necessary, as no previous studies have characterized the transient processes extensively. The changes in both long and short range order in the neat calcium carbonate material were monitored using wide-angle XRD patterns in conjunction with solid-state single-pulse ^{13}C and ^{1}H NMR spectra collected after 0, 8, 24, 48, and 120 hours of exposure to 76% relative humidity at 20°C. Wide-angle XRD measurements identify the different crystal structures present in the calcium carbonate materials, as well as probe the extent of long range (>10 nm) molecular order. By comparison, solid-state single-pulse ^{13}C and ^{1}H NMR measurements are sensitive to the local atomic bonding environments, relative quantities, and short-range (<1 nm) molecular order or disorder of distinct ^{13}C and ^{1}H sites in the calcium carbonate materials.

Immediately following the removal of the neat calcium carbonate material from the lyophilizer, corresponding XRD and NMR measurements were collected to characterize the material as it was synthesized (Figure 6, 0 hours). The XRD pattern exhibits two broad reflections of extremely low intensity centered at 30° and 45° 2θ which result from random scattering that is characteristic of an amorphous material. Complementarily, the inhomogeneously broadened signal (3.5 ppm fwhm) centered at 168.6 ppm in the single-pulse ^{13}C NMR measurements collected at 0 hours indicates that a broad distribution of ^{13}C atomic environments were present in the material, which is also characteristic of an amorphous solid, and the chemical shift is attributed to the average ^{13}C atomic environment

present in amorphous calcium carbonate.[34] Likewise, the broadened ^{1}H signals centered at 5.0 ppm (5 ppm fwhm) and 1.3 ppm (2 ppm fwhm) establish the presence of a wide distribution of ^{1}H sites in the material which can be attributed to the structural water and -OH groups found in amorphous calcium carbonate, respectively.[34] Altogether, the XRD and solid-state NMR measurements collected at 0 hours indicate that the material as-synthesized was amorphous calcium carbonate.

To induce controlled, reproducible crystallization of the neat amorphous calcium carbonate, the material was stored at 76% relative humidity and 20°C following removal from the lyophilizer. After 8 hours, a few hundred milligrams of the calcium carbonate was removed from the controlled environment and further XRD and NMR measurements were conducted to characterize the crystallization process (Figure 6, 8 hours). The wide-angle XRD pattern exhibits a single, narrow reflection of low intensity at 29° 2θ that is indexable to the [1 0 4] plane of calcite, however the aforementioned broad reflections centered at 30° and 45° 2θ remain, indicating that a significant amount of amorphous calcium carbonate was present in the material. Correspondingly, an additional signal (0.4 ppm fwhm) centered at 168.7 ppm is manifested in the single-pulse ^{13}C spectrum collected at 8 hours, which can be attributed to the single ^{13}C atomic environment present in calcite.[34] A significant amount of amorphous calcium carbonate remained in the material as evidenced by the intense, inhomogeneously broadened signal (3.3 ppm fwhm) centered at 168.6 ppm. To determine the relative amounts of each distinct ^{13}C site in the calcium carbonate material, Lorentzian line fits were applied to deconvolute the overlapping signals and then integrated to quantify the relative amounts of calcite and amorphous calcium carbonate. This analysis revealed that the material was composed of 2% of the single crystallographic site attributed to calcite and 98%

of the distribution of sites assigned to amorphous calcium carbonate (Table 1). The broadened ^{1}H signals centered at 5.0 ppm (2 ppm fwhm) and 1.3 ppm (2 ppm fwhm) remain in the single pulse ^{1}H spectrum, indicating that the structural water and -OH groups (respectively) associated with the amorphous calcium carbonate were still present in the material. However the intensity of the signal associated with the -OH groups and linewidth of the signal associated with the structural water have decreased slightly, indicating that the ^{1}H sites in the material were slightly more uniform as is consistent with amorphous calcium carbonate crystallizing to anhydrous crystalline calcium carbonate. In summary, the XRD and solid-state NMR measurements indicate that after 8 hours at 76% relative humidity, calcite crystals had begun to nucleate and grow in the amorphous calcium carbonate nanoparticles. Furthermore, in the absence of surface additives, the amorphous calcium carbonate nanoparticles began to crystallize to the most thermodynamically stable of the anhydrous crystalline polymorphs.

Once the neat calcium carbonate material was exposed to 76% relative humidity for 24 hours, additional material was removed to characterize the extent of crystallization using complementary XRD and NMR measurements (Figure 6, 24 hours). The broad reflections centered at 30° and 45° 2θ that were present in the XRD measurements at 8 hours are replaced by two sets of narrow reflections indexable to calcite and vaterite, indicating that the crystallization process of the neat amorphous calcium carbonate was complete by 24 hours. The calcite reflections have greater intensity in comparison with the vaterite reflections, signifying that there was a larger amount of calcite relative to vaterite in the crystallized calcium carbonate material. The single-pulse ^{13}C NMR measurements exhibit signals at 170.6 ppm, 169.5 ppm, and 168.7 ppm that are assigned to two ^{13}C atomic sites in vaterite

and the single ^{13}C atomic environment present in calcite, respectively,[34] confirming the presence of the crystalline polymorphs manifested in the XRD spectrum. Several recent publications have proposed explanations that could account for the two distinct ^{13}C atomic sites in vaterite established by solid-state ^{13}C NMR. Demichelis et. al. suggest that vaterite is a dynamic system in which CO_3^{2-} anions have "rotational freedom at room temperature" and therefore the resulting crystal structure of vaterite is an average of at least three minimum energy configurations.[9] Kabalah-Amitai et. al. propose a random distribution of two coexisting crystal structures with a major structure exhibiting hexagonal symmetry and a minor structure of unknown symmetry, which is consistent with the observation of two distinct vaterite signals.[11] It is notable that no aragonite was present in the material, as the ^{13}C signal would appear at a chemical shift of 171 ppm,[34] around 0.5 ppm downfield of the second vaterite signal, and it similarly is not present in any of the other ^{13}C measurements collected and presented in this thesis. It is known that the calcite and aragonite polymorphs have similar enthalpies (Figure 2a) so final polymorph selection is likely sensitive to subtle differences in the crystallization pathway. The linewidths for each of the calcite and vaterite signals are extremely narrow, with a full-width half-maximum (fwhm) of 0.3 ppm for calcite and 0.6 ppm and 0.5 ppm for the first (169.5 ppm) and second (170.6 ppm) ^{13}C atomic environments in vaterite, respectively. These narrow linewidths are indicative of a uniform local atomic order for each of the distinct crystallographic sites in the calcium carbonate material. The signals were again deconvoluted using Lorentzian line fits, establishing that the material was composed of 7% of the first ^{13}C atomic environment attributed to vaterite, 3% of the second ^{13}C atomic environment attributed to vaterite, and 90% of the ^{13}C atomic environment attributed to calcite after 24 hours of crystallization (Table 1). It is notable that

within a few percent error of the integration of the Lorentzian line fits applied to the spectrum, the crystallographic sites attributed to vaterite occurred in a 2:1 ratio. The ^{1}H signal centered at 1.3 ppm has disappeared, while the signal centered at 5.0 ppm has shifted to 4.6 ppm and narrowed considerably (0.3 ppm fwhm), indicating that the -OH groups associated with the disordered amorphous calcium carbonate have disappeared and that the water associated with the crystallized material has a more uniform atomic environment. Furthermore, the signal shift indicates that more electron density was present around the protons associated with water, which is consistent with the exclusion of structural water from the carbonate material. The only water remaining in the calcium carbonate material was likely surface water, which would interact to a lesser extent with the electron withdrawing oxygen groups in the carbonate anion. Taken in conjunction with the XRD measurements, the solid-state NMR measurements establish that after 24 hours at 76% relative humidity, no amorphous calcium carbonate remained in the nanoparticles. The thermodynamically stable calcite polymorph predominated (90% relative abundance), with trace amounts of kinetically metastable vaterite present in the material as well (10% relative abundance).

Additional measurements were collected for the neat calcium carbonate material after 48 hours and 120 hours in a controlled humidity and temperature environment. Comparing the wide-angle XRD patterns and the ^{13}C and ^{1}H NMR spectra acquired for the calcium carbonate material crystallized for 24 hours and those of the calcium carbonate material crystallized for 48 and 120 hours (Figure 6, 24 hours, 48 hours, and 120 hours), it is apparent that there are no changes in the reflections or intensities in the XRD patterns, as well as no variations in the chemical shifts, linewidths, and intensities of the signals present in the ^{13}C and ^{1}H NMR spectra. This indicates that the composition of the neat calcium carbonate

material reached a pseudo steady state after less than 24 hours of crystallization, with trace amounts of stabilized metastable vaterite present (10% relative abundance) in addition to the thermodynamically stable calcite (90% relative abundance).

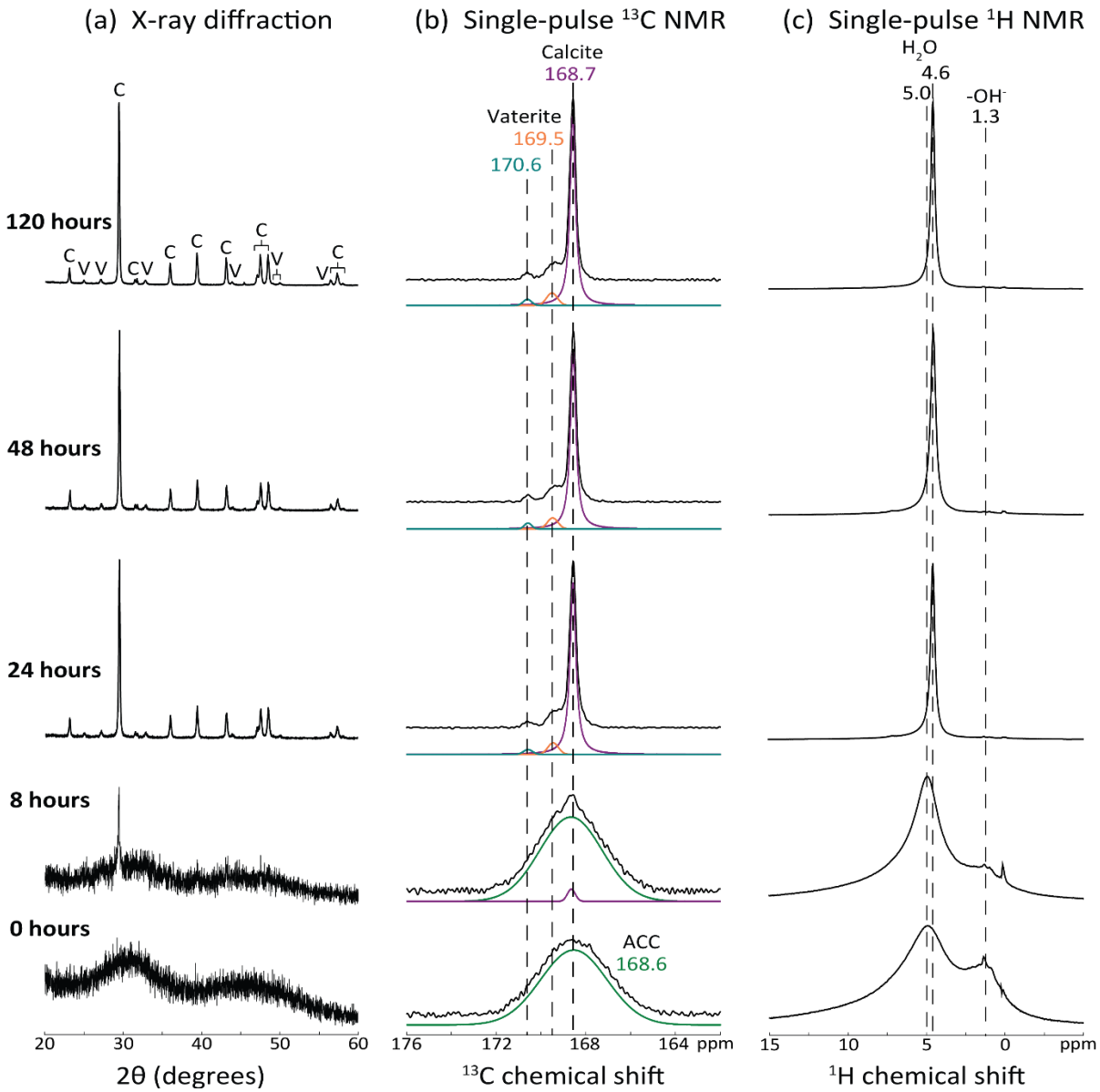

Figure 6. (a) Wide-angle powder XRD patterns, (b) solid-state single-pulse ^{13}C NMR spectra, and (c) solid-state single-pulse ^{1}H NMR spectra were acquired for amorphous calcium carbonate synthesized without surface additives and crystallized at 76% relative humidity for 0, 8, 24, 48, and 120 hours. XRD reflections were indexed to standard calcite (C) and vaterite (V) reflections. NMR spectra were acquired at 9.4 T, 298 K, and 10 kHz MAS and chemical shifts were referenced using a tetrakis(trimethylsilyl)silane (TKS) standard. Lorentzian line fits were applied to the ^{13}C NMR spectra to deconvolute the overlapping signals and quantify the relative amounts of each calcium carbonate polymorph.

Crystallization time (hrs)	Amorphous $CaCO_3$	Calcite	Vaterite Site 1	Vaterite Site 2
0	100%	-	-	-
8	98%	2%	-	-
24	-	90%	7%	3%
48	-	90%	7%	3%
120	-	90%	7%	3%

Table 1. Relative quantities of calcium carbonate polymorphs present in the calcium carbonate material prepared without surface additives and stored at 76% relative humidity for 0, 8, 24, 48, and 120 hours. Quantities are obtained from integration of Lorentzian line fits applied to solid-state single-pulse ^{13}C NMR spectra.

While single-pulse ^{13}C NMR measurements are inherently quantitative as the ^{13}C nuclei in the material are polarized directly, ^{13}C CP-MAS experiments employ polarization transfer to selectively detect ^{13}C nuclei that are dipole-dipole coupled to ^{1}H nuclei. The signal intensity in the cross polarization experiments is therefore based upon the molecular distance between the two NMR active nuclear isotopes, in this case ^{1}H nuclei and ^{13}C nuclei, in addition to the quantity of the isotopes that are adjacent to each other. By varying the amount of time that the polarization is transferred from the ^{1}H nuclei to the ^{13}C nuclei (contact time), information about different molecular distances as well as fast or slow relaxing species may be obtained. Solid-state ^{13}C CP-MAS NMR measurements were performed on the same neat calcium carbonate material after 0, 8, 24, 48, and 120 hours of storage at 76% relative humidity and 20°C. For these measurements, two contact times were selected; 500 ms (immediately adjacent nuclei, detects a greater quantity of fast relaxing species) and 3750 ms (adjacent nuclei, detects a greater quantity of slow relaxing species).

Solid-state ^{13}C CP-MAS NMR measurements were collected for the neat calcium carbonate material immediately after removal from the lyophilizer (Figure 7, 0 hours) to characterize the material as it was synthesized. For the measurements obtained with a 500 ms

contact time, the inhomogeneously broadened signal (3.4 ppm fwhm) centered at 168.6 ppm indicates that a wide distribution of ^{13}C atomic sites were proximate to ^{1}H atomic sites. This is consistent with the structural water and -OH groups found throughout the highly disordered amorphous calcium carbonate, and the chemical shift is consistent with the average chemical shift assigned to the ^{13}C environments in amorphous calcium carbonate. The measurements obtained with the 3750 ms contact time have a higher signal to noise ratio than those obtained with the 500 ms contact time, establishing that the increased contact time allowed for the detection of a larger number of ^{13}C atomic sites in the material. However the chemical shift of the signal (168.6 ppm) and the signal width (3.4 ppm fwhm) remain the same, indicating that the ^{13}C atomic sites that were adjacent to the ^{1}H atomic sites had a similar average electronic shielding as well as distribution at different molecular proximities. Furthermore, after 8 hours at 76% relative humidity (Figure 7, 8 hours), the signals for the 500 ms and 3750 ms contact time are unchanged with respect to their 0 hour counterparts, signifying that the structural water and -OH groups associated with amorphous calcium carbonate remained in the material and the molecular proximities of the ^{1}H and ^{13}C nuclei and distributions of ^{13}C atomic environments both remained the same.

Additional measurements were acquired after 24, 48, and 120 hours at a controlled relative humidity and temperature to characterize the ^{13}C atomic environments proximate to ^{1}H environments in the neat, fully crystalline calcium carbonate material. Comparing the ^{13}C CP-MAS NMR measurements acquired for the calcium carbonate material crystallized for 24 hours and those of the calcium carbonate material crystallized for 48 and 120 hours (Figure 7, 24 hours, 48 hours, and 120 hours), it is evident that the 500 ms contact time measurements and the 3750 ms contact time measurements are unchanged with respect to

chemical shift, linewidth, and intensity across the three time points, indicating that the material had reached a steady state. The peak intensities and linewidths for both the 500 ms contact time (1.3 ppm fwhm) and the 3750 ms contact time (1.3 ppm fwhm) have decreased from those observed at 0 hours and 8 hours (3.4 ppm fwhm), indicating that the molecular environments for the ^{13}C nuclei proximate to the ^{1}H nuclei had a more uniform order, and that the structural water and -OH groups associated with the disordered amorphous material were excluded from the now crystalline material. The only ^{1}H species remaining in the calcium carbonate material were associated with water (based on the single-pulse ^{1}H NMR measurements) that was likely physisorbed to the calcite and vaterite crystallites at the particle surface. Additionally, the chemical shift of the signal shifted from the 168.6 ppm observed at 0 and 8 hours to 168.8 ppm, indicating that the crystalline ^{13}C atomic environments that were proximate to the ^{1}H atomic environments were primarily those present in calcite (168.7 ppm). The signal shift and linewidth are identical for the 500 ms and 3750 ms contact times, establishing that the ^{13}C environments adjacent to the water were uniformly distributed across a range of distances.

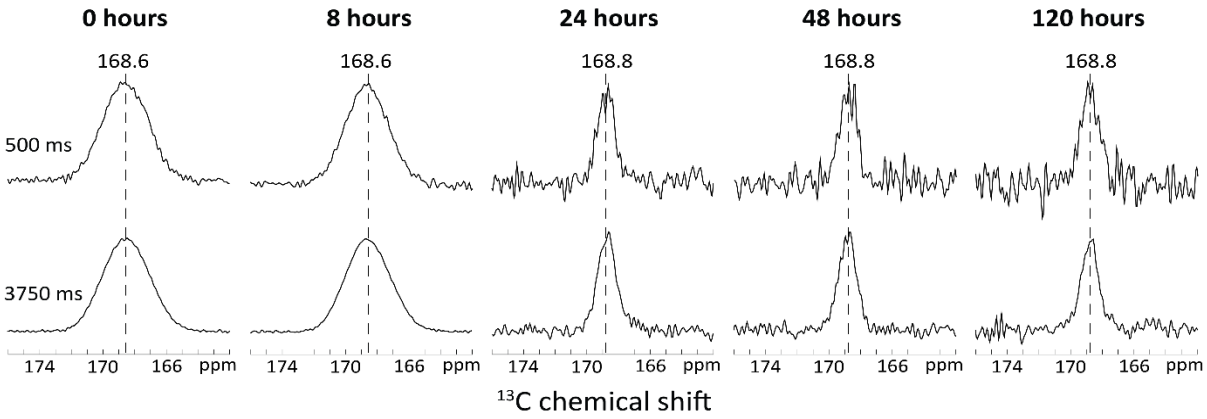

Figure 7. Solid-state ^{13}C CP-MAS NMR spectra were acquired for the same amorphous calcium carbonate synthesized without surface additives and crystallized at 76% relative humidity for 0, 8, 24, 48, and 120 hours as in Figure 6. NMR spectra were acquired for contact times of 500 ms and 3750 ms at 9.4 T, 298 K, and 10 kHz MAS and referenced using a tetrakis(trimethylsilyl)silane (TKS) standard.

To further characterize the crystalline calcium carbonate material (120 hours at 76% relative humidity), separate solid-state single-pulse ^{43}Ca measurements were conducted at the National High Magnetic Field Laboratory to probe the ^{43}Ca environments present (Figure 8). The single signal centered at 20 ppm indicates that the single ^{43}Ca environment attributed to calcite[35] was present in the material, which was expected to be the predominant calcium carbonate polymorph based on the separate solid-state single-pulse ^{13}C measurements and wide-angle XRD measurements conducted on a sample prepared and crystallized under the same conditions. The crystalline ^{43}Ca environments attributed to aragonite (-30 ppm)[35] and vaterite (10 ppm)[35] are not visible in this spectrum and it is evident that the sample did not contain appreciable amounts of amorphous material. This is also consistent with the solid-state single-pulse ^{13}C NMR measurements and XRD measurements conducted on a sample stored at 76% relative humidity for 120 hours, as only trace amounts of vaterite were present in the sample with no amorphous material or aragonite present within the limits of detection (<2%) (Figure 6). Furthermore, it is notable that no aragonite is present in any of the ^{43}Ca NMR measurements presented in this thesis. The differences observed between the two samples prepared and crystallized under identical conditions may be attributed to the fact that the crystallization of metastable calcium carbonate is inherently difficult to control, and agreement within +/- 10% of the relative abundance of the crystalline polymorphs present is adequate. The linewidth of the single signal (4 ppm fwhm) indicates that the ^{43}Ca environment was uniform, which is consistent with a highly crystalline calcite ^{43}Ca atomic environment.

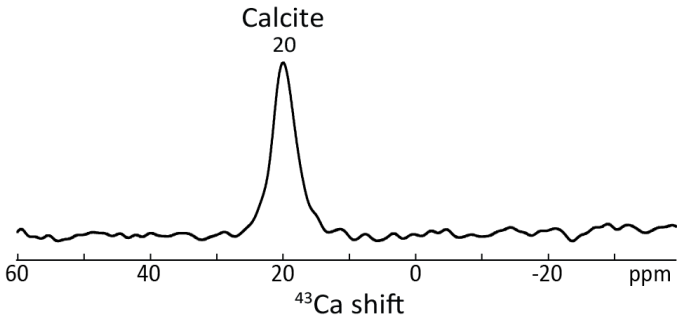

Figure 8. Solid-state single-pulse ^{43}Ca MAS NMR spectrum was acquired for amorphous calcium carbonate synthesized without surface additives and crystallized at 76% relative humidity for 120 hours. The NMR spectrum was acquired at 11.7 T, 298 K, and 5 kHz MAS and referenced using a 1.0 M $CaCl_2$ standard solution.

To characterize particle morphology and crystallinity, complementary SEM, TEM, and BET measurements were conducted on the neat calcium carbonate material prepared and crystallized under the same conditions (Figure 9). Measurements were obtained before (0 hours at 76% relative humidity) and after (120 hours at 76% relative humidity) crystallization. The scanning electron micrographs obtained for the material reveal that it was composed of aggregates of spherical nanoparticles that averaged 100 nm in diameter (Figure 9a, 0 hours). Although the particle morphology does not seem to change significantly based on the SEM images collected before and after crystallization, it does appear that an increased roughness in the spherical particles was present after crystallization (Figure 9a, 120 hours). Similarly, the bright-field transmission electron micrographs obtained before crystallization of the calcium carbonate material reveal that the particles were spherical with an average particle diameter of 100 nm (Figure 9b, 0 hours). The corresponding image collected after the samples were allowed to crystallize for 120 hours at 76% relative humidity reveals that some porosity was potentially present in the particle structures (Figure 9b, 120 hours). These nanopores could have been formed by the exclusion of water from the particle and crystallization of the surrounding carbonate material, resulting in areas of material depletion.

The BET surface area measurements contradict these observations - the initial surface area of the calcium carbonate material before crystallization was 25.7 ± 0.3 m^2/g while the surface area after crystallization is complete was around 16.7 ± 0.2 m^2/g. This discrepancy could arise from the fact that particle densification was occurring alongside the formation of the nanopores as the carbonate material crystallized, and that the decrease in surface area resulting from the densification process dominated the change in particle surface area such that the additional surface area provided by the nanopores was outweighed in comparison. An alternate explanation for the apparent nanoscale porosity is that the crystalline material aggregated and changed under the electron beam, resulting in the formation of the "nanopores" during imaging, therefore additional imaging is necessary to confirm these observations. The electron diffraction pattern for the corresponding bright-field image collected at 0 hours reveal that the calcium carbonate material as synthesized was completely amorphous as the electrons are deflected at random, forming rings of equal intensity (Figure 9c, 0 hours), therefore the dark-field image contained no discernable contrast. The selected area electron diffraction pattern collected for the fully crystalline calcium carbonate material exhibits scattering characteristic of a crystalline material (Figure 9c, 120 hours). Each of these diffraction spots in the electron diffraction pattern is characteristic of a crystallite that is oriented at random in the calcium carbonate material, and the spacing of the spots from the center of the pattern can be related to d-spacings present in the crystalline calcium carbonate polymorphs, thus establishing that the composition of the material was consistent with mixed calcium carbonate phases. Distinct spots in the pattern are indicative of larger single crystals in the calcium carbonate material, while rings of spots signify that the material was polycrystalline. The corresponding dark-field TEM supports these observations, as numerous

small randomly oriented crystallites (~2 nm in width) are visible alongside several larger crystalline regions (Figure 9d). High-resolution transmission electron microscopy was also performed on the fully crystalline sample that reveals the crystal lattice structures present in the material with the corresponding d-spacings from the electron diffraction (Figure 10).

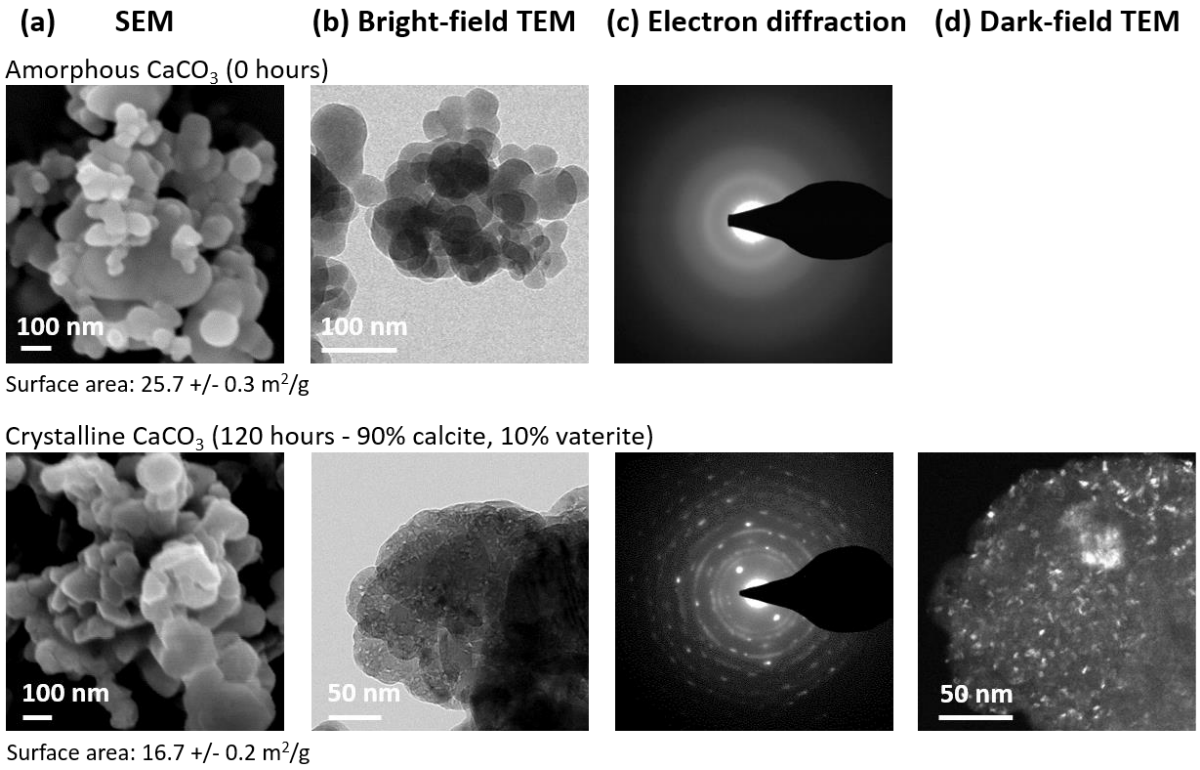

Figure 9. (a) Scanning electron micrographs, (b) bright-field transmission electron micrographs, (c) selected area electron diffraction patterns, and (d) dark-field transmission electron micrograph acquired for amorphous calcium carbonate synthesized without surface additives and crystallized at 76% relative humidity for 0 and 120 hours. Compositions are based upon single-pulse ^{13}C NMR measurements conducted on a sample prepared and crystallized under the same conditions (Figure 6 and Table 1). A dark-field TEM image was not collected at 0 hours as the material was diffracting electrons at random, therefore the dark-field image did not exhibit any contrast.

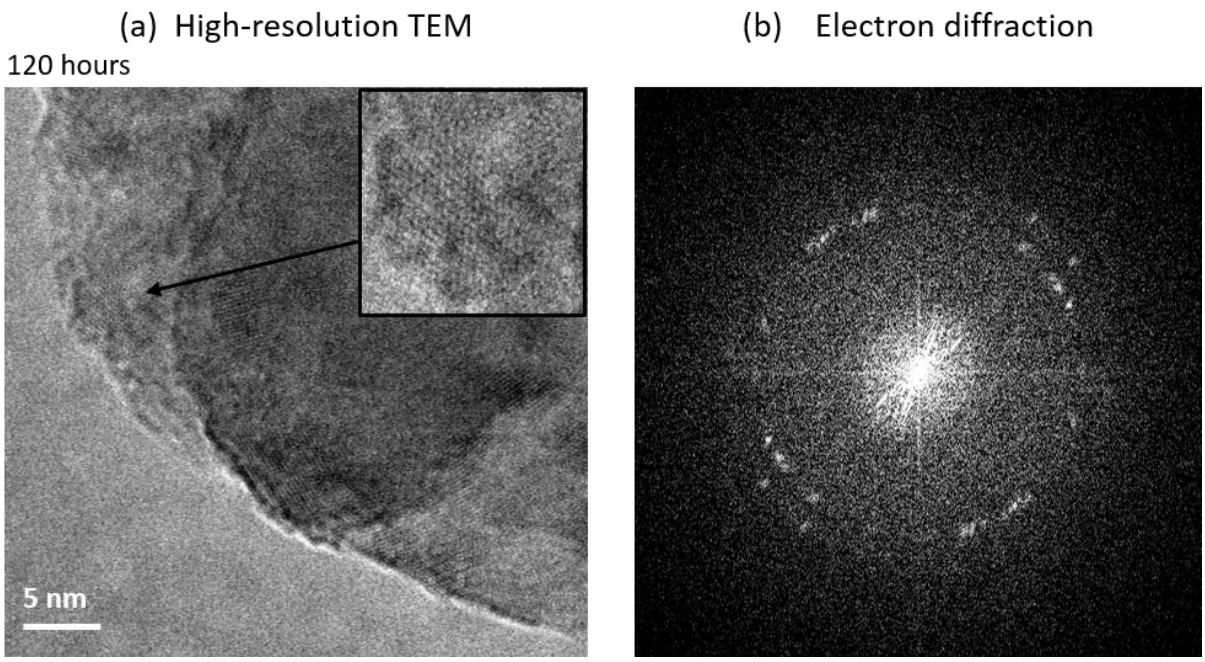

Figure 10. (a) High-resolution transmission electron micrograph and (b) corresponding selected area electron diffraction pattern acquired for amorphous calcium carbonate synthesized without surface additives and crystallized at 76% relative humidity for 120 hours.

To characterize the intermolecular interactions in the fully crystalline calcium carbonate material synthesized without surface additives, a 2D $^{13}C\{^{1}H\}$ HETCOR NMR spectrum was acquired (Figure 11a). A strong intensity correlation is observed between water (4.6 ppm) and the average carbonate environment (168.8 ppm), which is consistent with water that was excluded from the crystalline calcium carbonate material and adsorbed to the surface of the particles (Figure 11b). The spectrum was collected after crystallization was complete to provide a comparison with spectra collected for calcium carbonate with saccharide surface additives at the same time point. Spectra were not collected for the fully amorphous material synthesized with and without surface additives as it was established that structural hydroxyl groups were present in amorphous calcium carbonate that could provide a false indication of hydrogen bonding between the surface additives and calcium carbonate particles.

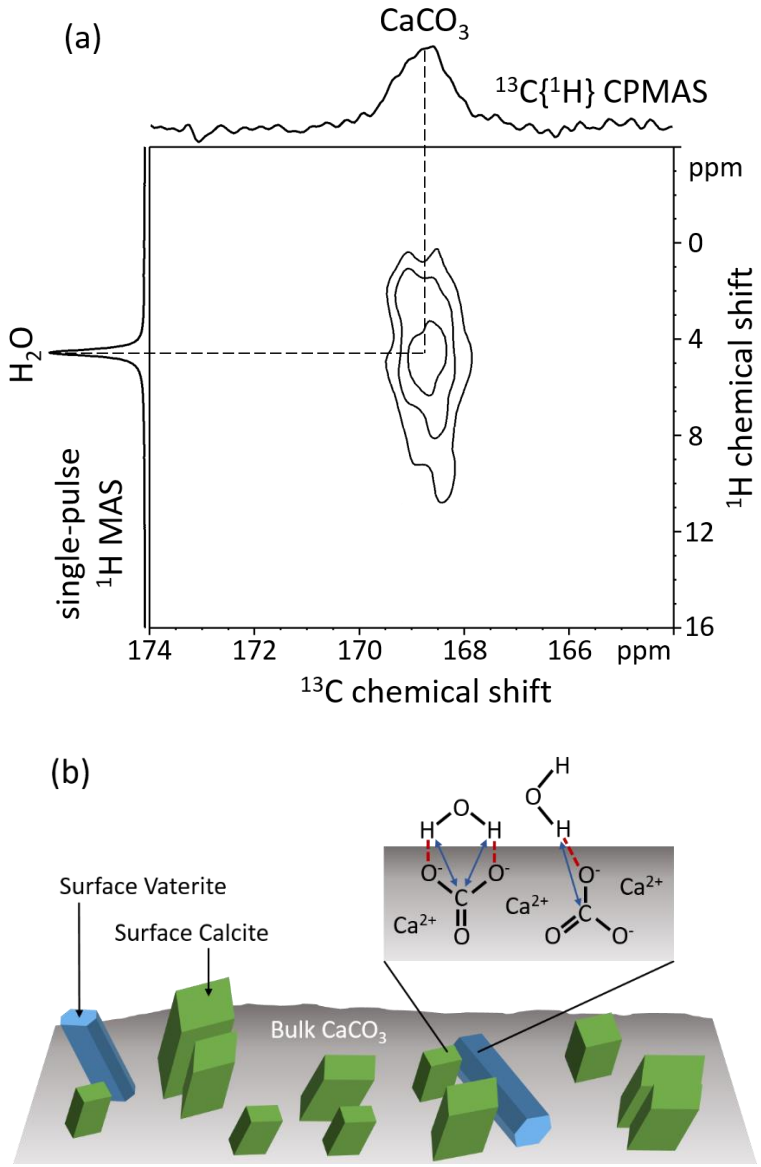

Figure 11. (a) Solid-state 2D $^{13}C\{^{1}H\}$ HETCOR NMR spectrum acquired for amorphous calcium carbonate synthesized without surface additives and crystallized at 76% relative humidity for 120 hours. 1D ^{13}C CP-MAS and single-pulse ^{1}H MAS spectra displayed along the horizontal and vertical axes, respectively. (b) Depiction of the calcium carbonate particle surface resulting from the crystallization of amorphous calcium carbonate without surface additives present.

3.2. Crystallization of amorphous calcium carbonate with adsorbed saccharides

3.2.1. Glucose, a reducing monosaccharide

Glucose (reducing monosaccharide) was selected as a surface additive of potential interest, taking inspiration from the stabilizing interactions of biological polysaccharides (chitosan and chitin) with amorphous calcium carbonate particle surfaces in biological organisms. Samples of calcium carbonate material were synthesized, crystallized, and characterized using the same procedures as described in the previous section, however a glucose adsorbate was applied in situ immediately following particle precipitation. As before, wide-angle powder XRD was used to characterize the extent of long range order and the crystalline calcium carbonate polymorphs, while single-pulse ^{13}C and ^{1}H NMR measurements were collected to probe the extents of short range molecular order, relative quantities of the calcium carbonate polymorphs, and distinct ^{13}C and ^{1}H atomic environments present in the material.

After removal of the material from the lyophilizer, XRD and solid-state ^{13}C and ^{1}H NMR measurements were obtained for the calcium carbonate material prepared with a glucose surface adsorbate to characterize the material as it was synthesized (Figure 12, 0 hours). The XRD pattern displays two broad, low-intensity reflections, the first centered at 30° and the second at 45° 2θ, which are characteristic of the random scattering of x-rays by an amorphous material. Complimentarily, the single-pulse ^{13}C NMR spectrum collected at 0 hours contains an inhomogeneously broadened signal (3.5 ppm fwhm) centered at 168.6 ppm which indicates that a broad distribution of ^{13}C atomic environments were present in the material. This distribution is characteristic of an amorphous material, while the chemical shift of 168.6 ppm corresponds to the average ^{13}C atomic environment present in amorphous

calcium carbonate. With regards to the single-pulse ^{1}H NMR, the broadened ^{1}H signals centered at 5.0 ppm (6 ppm fwhm) and 1.3 ppm (2 ppm fwhm) similarly establish the presence of a wide distribution of ^{1}H sites in the material. The signal at 5.0 ppm can be attributed to the structural water present in amorphous calcium carbonate, while the signal centered at 1.3 ppm corresponds to the -OH groups found in amorphous calcium carbonate and in the glucose additive. The comprehensive XRD and solid-state NMR measurements indicate that the calcium carbonate material as-synthesized was completely amorphous.

Following lyophilization, the calcium carbonate material with a glucose surface additive was stored at 20°C and 76% relative humidity as regulated by a saturated NaCl solution to induce crystallization. The crystallization process was monitored at the same time points as for the calcium carbonate material synthesized without additive; 8 hours, 24 hours, 48 hours, and 120 hours. No differences in the XRD patterns and the single-pulse ^{13}C NMR measurements for the 0 hour, 8 hour, and 24 hour time points are observed within the sensitivity of the measurements (Figure 12, 0 hours, 8 hours, 24 hours). The two broad reflections indicative of random scattering remain in the diffraction patterns, and the linewidth and signal shift do not change appreciably for the single signal in the ^{13}C NMR spectra. This indicates that the amorphous calcium carbonate material was kinetically stabilized by the glucose surface additive, as in the absence of surface additives the metastable amorphous material began to crystallize to calcite at 8 hours and was fully crystalline by 24 hours at 76% relative humidity. This delay in the onset of the crystallization process potentially resulted from electrostatic interactions of surface Ca^{2+} species with deprotonated glucose hydroxyl groups, or from hydrogen bonding of surface CO_3^{2-} species with glucose hydroxyl groups (Figure 13). It should be noted that the pKa of glucose is

12.28,[36] while the synthesis pH was 12.7 when the adsorbate was added which would indicate that both protonated and deprotonated glucose hydroxyl groups were present in solution. Furthermore, glucose is a known cryoprotectant in biological organisms that reduces cellular water loss,[37] and it is possible that the addition of glucose to the particle surface similarly reduced the loss of structural water, thus slowing the crystallization process and stabilizing the disordered amorphous material. Although the XRD and ^{13}C NMR measurements do not show measureable differences for the first three time points, the single-pulse ^{1}H NMR measurements indicate that the sample was still crystallizing slowly. The linewidth for the structural water signal at 5.0 ppm decreases slightly (5 ppm fwhm), and the signal corresponding to structural hydroxyl and glucose hydroxyl groups decreases in intensity. Both of these changes indicate that the calcium carbonate material with a glucose surface additive was becoming marginally more ordered over a period of 24 hours, although the material remained fully amorphous based on ^{13}C NMR and XRD measurements.

After the calcium carbonate material with a glucose surface adsorbate was exposed to 76% relative humidity for 48 hours (Figure 12, 48 hours), crystallization was manifested in the material. The primary reflection of calcite (29° 2θ, [1 0 4] plane) is visible in the wide-angle XRD pattern, however significant amounts of amorphous calcium carbonate were still present in the material based on the broad reflections centered at 30° and 45° 2θ. Complimentarily, the single-pulse ^{13}C spectrum collected at 48 hours exhibits an additional signal (0.4 ppm fwhm) centered at 168.7 ppm. This signal can be attributed to the single ^{13}C atomic environment present in calcite, however the inhomogeneously broadened signal (3.3 ppm fwhm) centered at 168.6 ppm corresponding to amorphous calcium carbonate still predominates. The overlapping signals were deconvoluted using Lorentzian line fits and the

relative amounts of the distinct ^{13}C sites were quantified (Table 2). Integration of these fits reveals that the material was composed of 2% of the single crystallographic site attributed to calcite and 98% of the distribution of sites assigned to amorphous calcium carbonate. The single-pulse ^{1}H measurements indicate that a significant amount of structural water remained in the amorphous material after 48 hours of crystallization based on the broadened ^{1}H signal centered at 5.0 ppm (5 ppm fwhm). Furthermore, the ^{1}H signal centered at 1.3 ppm (2 ppm fwhm) indicates that structural hydroxyl groups were present in the amorphous calcium carbonate material with additional intensity resulting from glucose hydroxyl present in the carbonate material. In comparison to the signals observed in the previous ^{1}H measurements, the intensities, chemical shifts, and linewidths of both signals have not changed appreciably. In summary, both wide angle XRD and solid-state NMR measurements indicate that after 48 hours at 76% relative humidity, calcite crystals had begun to nucleate and grow in the amorphous calcium carbonate nanoparticles prepared with a glucose surface additive. Furthermore, in the presence of a glucose (reducing saccharide) surface additive, the amorphous calcium carbonate nanoparticles will begin to crystallize to the most thermodynamically stable of the anhydrous crystalline polymorphs.

Following exposure to 76% relative humidity for 120 hours (Figure 12, 120 hours), the XRD pattern obtained for the calcium carbonate material prepared with a glucose surface additive exhibits two sets of narrow reflections that are indexable to calcite and vaterite. The calcite reflections have greater intensity in comparison with the vaterite reflections, as seen with the sample crystallized without surface additive, indicating that there was a larger amount of calcite relative to vaterite in the crystallized calcium carbonate material. However, the vaterite reflections have greater intensity than previously observed in the sample

crystallized without additive, indicating that more of the metastable vaterite polymorph was formed. Correspondingly, the single-pulse ^{13}C NMR measurements indicate that crystalline calcite and vaterite were present in the material. Signals at 170.6 ppm, 169.5 ppm, and 168.7 ppm that are assigned to two ^{13}C atomic sites in vaterite and the single ^{13}C atomic environment present in calcite, respectively, are manifested in the ^{13}C spectrum. The narrow linewidths (0.5 ppm fwhm, 0.7 ppm fwhm, and 0.4 ppm fwhm, respectively) for each of these signals is indicative of a uniform local atomic order for each of the distinct sites in the calcium carbonate material, consistent with a fully crystalline material. The integration of the deconvoluted signals establishes that the material was composed of 23% of the first ^{13}C atomic environment attributed to vaterite, 10% of the second ^{13}C atomic environment attributed to vaterite, and 67% of the ^{13}C atomic environment attributed to calcite. Again, within a few percent error of the integration of the Lorentzian line fits applied to the spectrum, the relative populations of the crystallographic sites attributed to vaterite occurred in a 2:1 ratio. The ^{1}H NMR measurements also indicate that the calcium carbonate material had become more ordered. The ^{1}H signal at 1.3 ppm associated with the structural -OH groups in the amorphous material and potentially with the -OH groups present in the glucose surface additive has decreased in intensity, consistent with the crystallization of the amorphous material. Furthermore, the ^{1}H signal corresponding to the structural water has shifted from 5.0 ppm to 4.8 ppm and narrowed considerably (2 ppm fwhm), indicating that the water associated with the crystalline material had a more uniform atomic environment as expected. As previously discussed, the signal shift is likely due to the exclusion of structural water from the carbonate material as it crystallized, leaving only surface water. Altogether, the XRD and solid-state NMR measurements establish that after 120 hours at 76% relative

humidity, no amorphous calcium carbonate remained in the calcium carbonate nanoparticles synthesized with a glucose surface additive.

To summarize the significant findings from this series of XRD and solid-state NMR measurements, the onset of crystallization for the amorphous calcium carbonate material crystallized in the presence of a glucose surface additive was delayed in comparison with the same material crystallized without a surface additive. Crystallization was first manifested after 48 hours at 76% relative humidity in the presence of the glucose surface additive, in comparison to 8 hours without any surface additive present. Furthermore, although the thermodynamically stable calcite polymorph predominated in the fully crystalline calcium carbonate material with a glucose adsorbate (67% relative abundance), the kinetically metastable vaterite polymorph was present in significant quantities (33% relative abundance). Comparing these results with those for the amorphous calcium carbonate crystallized without a surface additive (90% calcite, 10% vaterite), it is evident that the glucose surface additive stabilized larger amounts the kinetically metastable vaterite polymorph. In conclusion, the glucose (reducing sugar) surface additive delayed the onset of crystallization in amorphous calcium carbonate, as well as favored the formation of greater amounts of metastable vaterite.

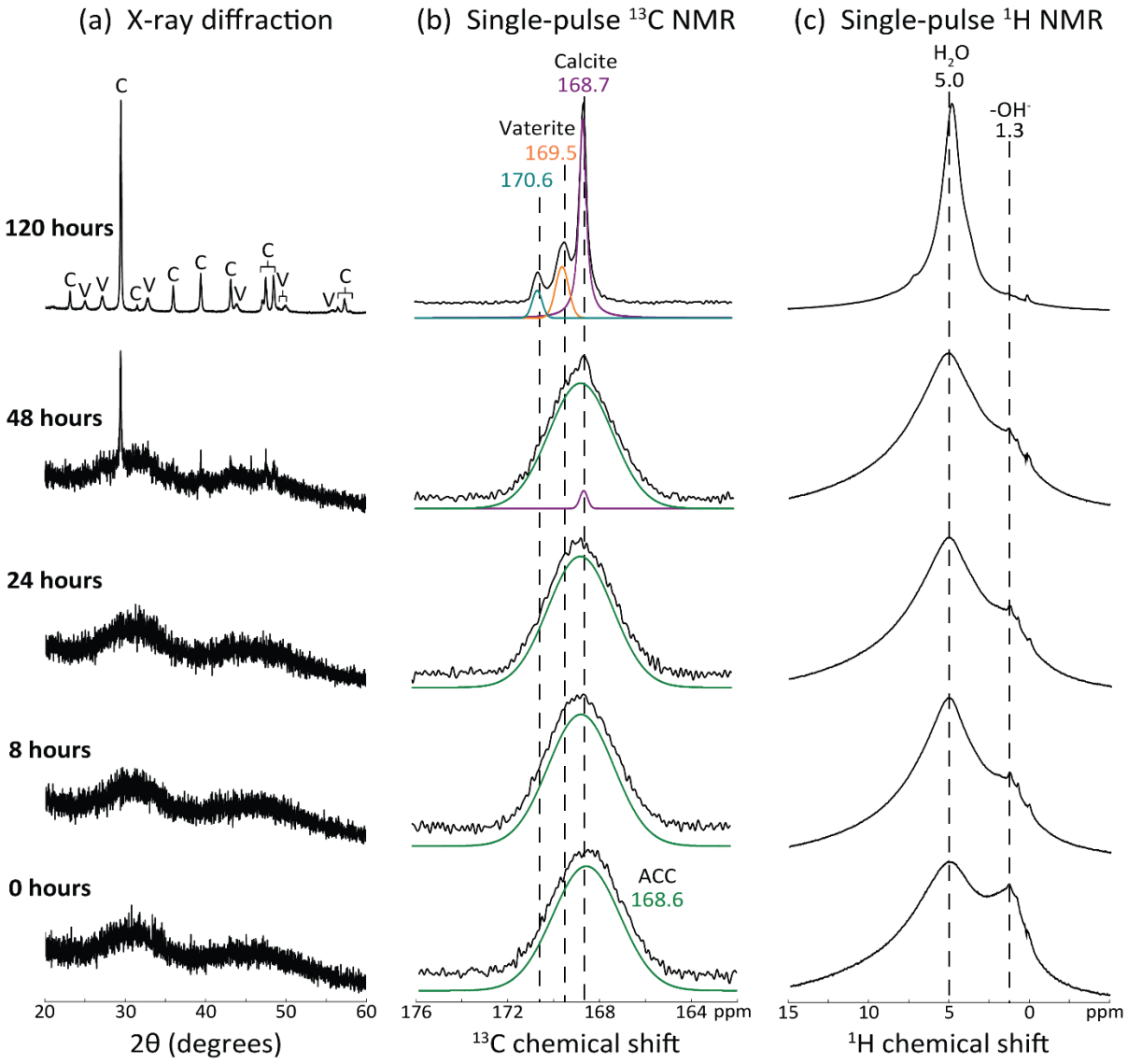

Figure 12. (a) Wide-angle powder XRD patterns, (b) solid-state single-pulse ^{13}C NMR spectra, and (c) solid-state single-pulse ^{1}H NMR spectra were acquired for amorphous calcium carbonate synthesized with a glucose surface additive and crystallized at 76% relative humidity for 0, 8, 24, 48, and 120 hours. XRD reflections were indexed to standard calcite (C) and vaterite (V) reflections. NMR spectra were acquired at 9.4 T, 298 K, and 10 kHz MAS and chemical shifts were referenced using a tetrakis(trimethylsilyl)silane (TKS) standard. Lorentzian line fits were applied to the ^{13}C NMR spectra to deconvolute the overlapping signals and quantify the relative amounts of each calcium carbonate polymorph.

Crystallization time (hrs)	Amorphous $CaCO_3$	Calcite	Vaterite Site 1	Vaterite Site 2
0	100%	-	-	-
8	100%	-	-	-
24	100%	-	-	-
48	98%	2%	-	-
120	-	67%	23%	10%

Table 2. Relative quantities of calcium carbonate polymorphs present in the calcium carbonate material prepared with a glucose surface additive and stored at 76% relative humidity for 0, 8, 24, 48, and 120 hours. Quantities are obtained from integration of Lorentzian line fits applied to solid-state single-pulse ^{13}C NMR spectra.

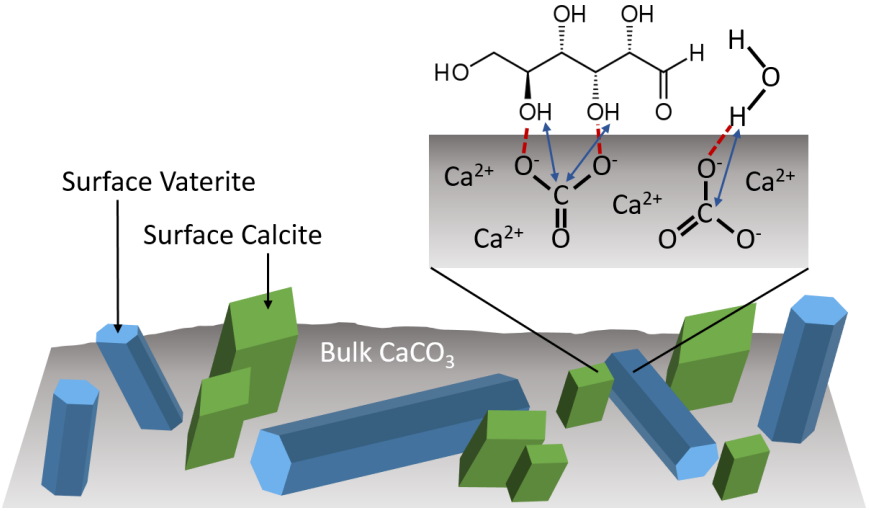

Figure 13. Depiction of the interaction of glucose (reducing saccharide) with the crystal structures present at the calcium carbonate particle surface.

Solid-state ^{13}C CP-MAS NMR measurements were performed on the same calcium carbonate material with a glucose adsorbate using to characterize the ^{13}C environments in molecular proximity to ^{1}H sites at different points in the crystallization process. Immediately after removal from the lyophilizer (Figure 14, 0 hours) the measurements obtained with a 500 ms contact time contain a single inhomogeneously broadened signal (3.4 ppm fwhm) centered at 168.6 ppm indicating that a wide distribution of ^{13}C atomic sites are proximate to ^{1}H atomic sites. The signal intensity results primarily from the molecular proximity between

the structural water and -OH groups found throughout the highly disordered ACC and the carbonate anions, while the chemical shift is consistent with the average chemical shift assigned to the ^{13}C environments in amorphous calcium carbonate. This signal could also contain intensity resulting from the protons within the saccharide molecules that were proximate to surface carbonate species. Increasing the contact time from 500 ms to 3750 ms contact time increases the signal to noise ratio, however the chemical shift of the signal (168.6 ppm) and the signal width (3.4 ppm fwhm) remain the same within the sensitivity of the measurements. This establishes that the increased contact time allowed for the detection of a larger number of ^{13}C atomic sites in the material and that the ^{13}C atomic sites adjacent to the ^{1}H atomic sites had a similar average electronic shielding as well as distribution at different molecular proximities. Furthermore, the signals for the 500 ms and 3750 ms contact time are unchanged across a 48 hour time period (Figure 14, 0 hours, 8 hours, 24 hours, 48 hours), signifying that the structural water and -OH groups associated with amorphous calcium carbonate and the glucose surface additive remained in the material and the molecular proximities of the ^{1}H and ^{13}C nuclei and distributions of ^{13}C atomic environments both remained the same.

The ^{13}C CP-MAS NMR spectrum acquired for the calcium carbonate material crystallized with a glucose surface additive for 120 hours differs slightly from those obtained for the first four timepoints (Figure 14, 120 hours). The peak intensities and linewidths for the 3750 ms contact time (1.7 ppm fwhm) and 500 ms contact time (1.7 ppm fwhm) have decreased and the center of the signal has shifted to 168.9 ppm, indicating that the molecular environments for the ^{13}C nuclei proximate to the ^{1}H nuclei had a more uniform order and an average ^{13}C atomic environment between that of calcite and vaterite. The observed decreases

in signal intensity result from the exclusion of the structural water and -OH groups associated with the disordered amorphous material. Any water remaining in the material was likely physisorbed to the calcite and vaterite crystallites at the particle surface. The shift in the average ^{13}C atomic environment is not observed for the calcium carbonate material crystallizing without surface additive present, which could indicate that once the structural water and hydroxyl groups in the carbonate material are depleted by crystallization, a larger portion of the CP signal results from the protons on saccharide molecules that are adjacent to carbonate anions at the particle surface. The saccharide molecules are likely associated with a more metastable phase of calcium carbonate, such as vaterite, which could result in the observed signal shift.

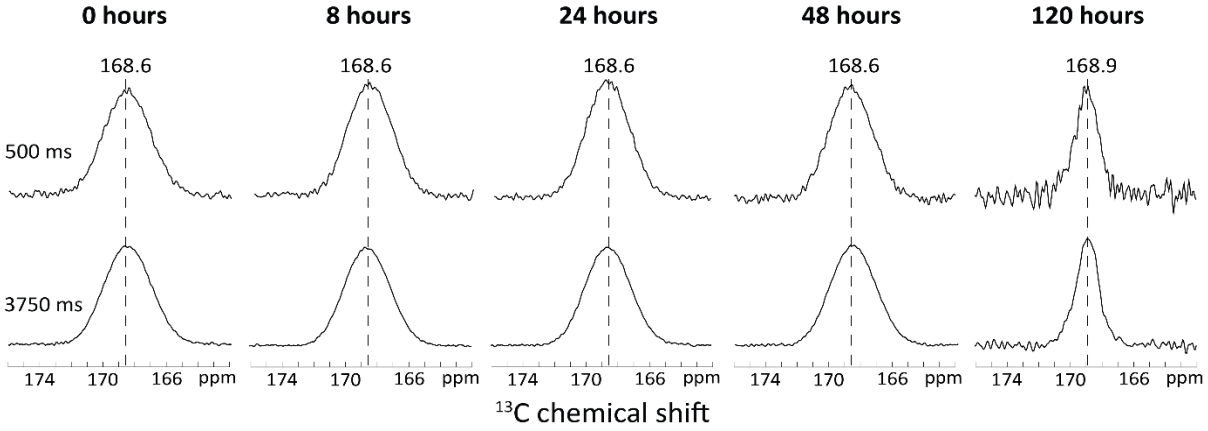

Figure 14. Solid-state ^{13}C CP-MAS NMR spectra were acquired for the same amorphous calcium carbonate synthesized with a glucose surface additive and crystallized at 76% relative humidity for 0, 8, 24, 48, and 120 hours as in Figure 12. NMR spectra were acquired for contact times of 500 ms and 3750 ms at 9.4 T, 298 K, and 10 kHz MAS and referenced using a tetrakis(trimethylsilyl)silane (TKS) standard.

To further characterize the fully crystalline calcium carbonate material prepared with a glucose surface additive (120 hours at 76% relative humidity), separate solid-state single-pulse ^{43}Ca measurements were conducted at the National High Magnetic Field Laboratory (Figure 15). The measurements indicate that two distinct ^{43}Ca environments were present in

the material and the separate signals can be deconvoluted using Lorentzian line fits (^{43}Ca is only a weakly quadrupolar nucleus and therefore Lorentzian fits are applicable). The more intense, narrow (7 ppm fwhm) signal centered at 19 ppm indicates that the predominant ^{43}Ca environment that was present in the sample can be attributed to calcite, which is expected based on the separate solid-state single-pulse ^{13}C measurements and wide-angle XRD measurements conducted on a sample prepared and crystallized under the same conditions. The less intense, broadened signal (16 ppm fwhm) centered at 5 ppm corresponds to the average ^{43}Ca environment present in vaterite, which was also present in significant quantities based on single-pulse ^{13}C measurements and wide-angle XRD measurements. It is notable that although the ^{13}C measurements reveal that crystalline vaterite has two distinct ^{13}C sites with relatively uniform distributions (0.5 ppm and 0.7 ppm fwhm), there is only one ^{43}Ca signal attributed to vaterite and it is extremely broadened. It would follow that there are at least two distinct ^{43}Ca sites in vaterite, and the single broadened signal in the measurements is likely composed of multiple overlapping signals resulting from ^{43}Ca sites which have similar average electronic shielding. The integration of the Lorentzian deconvolutions reveals that the calcium carbonate material fully crystallized in the presence of a glucose surface additive was composed of 66% of the single ^{43}Ca site attributed to calcite and 34% of the distribution of ^{43}Ca sites attributed to vaterite. In comparison, the relative populations indicated by the single-pulse ^{13}C NMR measurements (Figure 12, 120 hours) were 67% of the single ^{13}C site assigned to calcite and 33% of the two ^{13}C sites assigned to vaterite (Table 2).

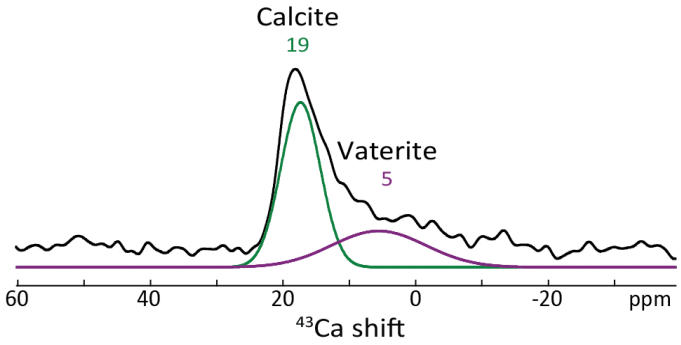

Figure 15. Solid-state single-pulse ^{43}Ca MAS NMR spectrum was acquired for amorphous calcium carbonate synthesized with a glucose surface additive and crystallized at 76% relative humidity for 120 hours. NMR spectrum was acquired at 11.7 T, 298 K, and 5 kHz MAS and referenced using a 1.0 M $CaCl_2$ standard solution.

Complementary SEM, TEM, and BET measurements were conducted on a calcium carbonate material prepared with a glucose adsorbate and crystallized under the same conditions (Figure 16) to characterize particle morphology and crystallinity. Measurements were obtained before (0 hours at 76% relative humidity) and after (120 hours at 76% relative humidity) crystallization. The initial SEM images reveal that the amorphous material was composed of aggregates of spherical nanoparticles averaging 100 nm in diameter, and the SEM images obtained for the crystalline material after 120 hours show that the morphology and particle diameter did not change significantly (Figure 16a). Likewise, the bright-field transmission electron micrograph obtained before crystallization of the calcium carbonate material reveals that the particles were roughly spherical, as does the corresponding image collected after the samples were allowed to crystallize for 120 hours at 76% relative humidity (Figure 16b). The increased particle roughness (and tentative nanoporosity) observed for the amorphous calcium carbonate crystallized without surface additive is not observed in the presence of a glucose surface additive, potentially due to the cryoprotectant functionality of the glucose molecule that inhibited the exclusion of structural water from the particles. The BET surface area measurements allude to particle densification as the material crystallizes;

the initial surface area of the calcium carbonate material with a glucose adsorbate was 33.9 ± 0.2 m^2/g while the surface area after crystallization was around 28.5 ± 0.2 m^2/g. These surface areas are noticeably different from the surface areas measured for the amorphous material crystallized without surface additives, which were 25.7 ± 0.3 m^2/g and 16.7 ± 0.2 m^2/g, respectively. The observed differences could arise from the fact that the glucose inhibited aggregation of the amorphous calcium carbonate particles, thus increasing the measured surface area. The corresponding electron diffraction patterns for the bright-field TEM images (Figure 16c) indicate that the calcium carbonate material as synthesized was completely amorphous, while the pattern collected after the calcium carbonate material was stored at 76% relative humidity for 120 hours exhibits regular scattering characteristic of a polycrystalline material with some large single crystals, with d-spacings consistent with mixed crystalline calcium carbonate phases. The dark-field TEM image supports these observations, as numerous small crystallites of a few nanometers in width are visible alongside several crystalline regions that are much larger in size (10-50 nm) (Figure 16d).

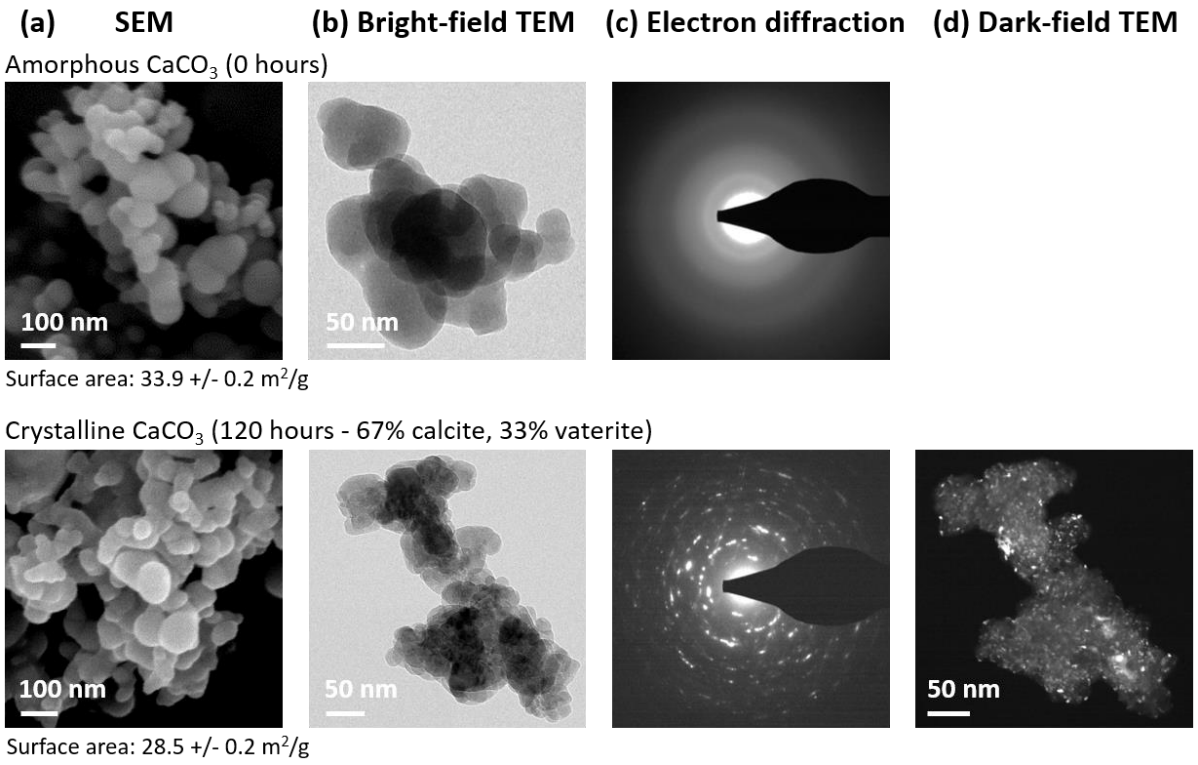

Figure 16. (a) Scanning electron micrographs, (b) bright-field transmission electron micrographs, (c) selected area electron diffraction patterns, and (d) dark-field transmission electron micrograph acquired for amorphous calcium carbonate synthesized with a glucose surface additive and crystallized at 76% relative humidity for 0 and 120 hours. Compositions are based upon single-pulse ^{13}C NMR measurements conducted on a sample prepared and crystallized under the same conditions (Figure 12 and Table 2). A dark-field TEM image was not collected at 0 hours as the material was diffracting electrons at random, therefore the dark-field image did not exhibit any contrast.

3.2.2. Sucrose, a non-reducing disaccharide

To provide maximum contrast to the crystallization processes of amorphous calcium carbonate in the presence of a reducing saccharide (glucose) surface additive, a non-reducing saccharide (sucrose) surface additive was selected for further study, again taking inspiration from the stabilizing interactions of biological polysaccharides (chitosan and chitin) with amorphous calcium carbonate particle surfaces in biological organisms. Samples of calcium carbonate material were synthesized and crystallized using the same procedure as described previously, however a sucrose surface adsorbate was applied in situ immediately following particle precipitation. As before, wide-angle powder XRD was used to characterize the extent of long range order and the crystalline calcium carbonate polymorphs, while single-pulse ^{13}C and ^{1}H NMR measurements were collected to probe the extents of short range molecular order, relative quantities of the calcium carbonate polymorphs, and distinct ^{13}C and ^{1}H atomic environments present in the material.

To characterize the material as synthesized, XRD patterns in conjunction with solid-state single-pulse ^{13}C and ^{1}H NMR measurements were collected after removal of the material from the lyophilizer (Figure 17, 0 hours). These measurements reveal that the material as synthesized was amorphous calcium carbonate. The wide-angle XRD pattern exhibits two broad, low-intensity reflections which are characteristic of the random scattering of X-rays from an amorphous material. Furthermore, a single, inhomogeneously broadened signal centered at 168.6 ppm is present in the solid-state single-pulse ^{13}C NMR spectrum collected at 0 hours. The signal shift corresponds to the average ^{13}C environment present in amorphous calcium carbonate, while the broadened signal (3.5 ppm fwhm) indicates that a wide distribution of ^{13}C atomic environments were present in the material, again consistent with an

amorphous sample. The single-pulse ^{1}H NMR measurements are consistent with the ^{13}C NMR measurements; two broadened ^{1}H signals are present in the spectrum, the first centered at 5.0 ppm (6 ppm fwhm) is assigned to the structural water present in amorphous calcium carbonate and the second centered at 1.3 ppm (2 ppm fwhm) corresponds to the -OH groups found in amorphous calcium carbonate and in the sucrose surface additive. The inhomogeneous broadening of these two signals establishes the presence of a wide distribution of ^{1}H sites in the material. Altogether, the wide-angle XRD and solid-state NMR measurements indicate that the synthesized material was amorphous calcium carbonate with a sucrose surface additive.

Following lyophilization, the crystallization process of the calcium carbonate material synthesized with a sucrose adsorbate was monitored after 8 hours, 24 hours, 48 hours, and 120 hours of exposure to 76% relative humidity (Figure 17, 8 hours, 24 hours, 48 hours, 120 hours). The XRD patterns and ^{13}C NMR measurements obtained at 8 and 24 hours exhibit no differences (within the sensitivity of the measurements) to those obtained initially at 0 hours. The broad reflections indicative of random scattering remain in the diffraction patterns, and the linewidth and signal shift do not change appreciably for the signals in the ^{13}C NMR spectra. Given that in the absence of surface additives amorphous calcium carbonate began to crystallize to calcite after 8 hours and was fully crystalline after 24 hours, it is evident that the amorphous material was stabilized by the sucrose surface additive. As with the glucose surface additive, delay in the onset of the crystallization process potentially resulted from electrostatic interactions of surface Ca^{2+} species with deprotonated sucrose hydroxyl groups, or from hydrogen bonding of surface CO_3^{2-} species with sucrose hydroxyl groups (Figure 21 b). It should be noted that the pKa of sucrose is 12.62,[36] while the synthesis pH was 12.7

when the adsorbate was added which would indicate that both protonated and deprotonated sucrose hydroxyl groups were present in solution. Furthermore, sucrose is also commonly used as a cryoprotectant,[38] and as with glucose, could have inhibited the exclusion of structural water from the calcium carbonate particles thus stabilizing the disordered ACC. Although the XRD and ^{13}C NMR measurements indicate that the calcium carbonate prepared with a sucrose surface additive remained fully amorphous for a period of 24 hours at 76% relative humidity, the single-pulse ^{1}H NMR measurements reveal that the material was still changing. The ^{1}H signal linewidths and shifts remain the same across the first three time points, however the intensity of the ^{1}H signal corresponding to the hydroxyl groups present in the sample decreases after 8 hours at 76% relative humidity. This indicates that the sample was becoming slightly more ordered over a period of 8 hours, as a large fraction of the hydroxyl sites present in the material were associated with the amorphous calcium carbonate. In summary, XRD and solid-state NMR measurements indicate that the crystallization process of amorphous calcium carbonate was delayed by the presence of a sucrose (non-reducing saccharide) surface additive.

Following 48 hours of exposure to 76% relative humidity (Figure 17, 48 hours), XRD and ^{13}C and ^{1}H solid-state NMR measurements indicate that the calcium carbonate material synthesized with a sucrose adsorbate contained crystalline calcium carbonate. Reflections indexable to calcite and vaterite are visible in the wide-angle XRD pattern, however the reflections are of low intensity, indicating that the material was likely not fully crystalline. Interestingly, the vaterite reflections are of greater intensity than the calcite reflections, which reveals that the calcium carbonate material prepared with a sucrose surface additive began to crystallize to a metastable polymorph of calcium carbonate in more significant amounts than

observed with the glucose surface additive or no surface additive. Complimentarily, the single-pulse ^{13}C spectrum collected at 48 hours exhibits four signals when properly deconvoluted by Lorentzian line fits. An inhomogeneously broadened signal corresponding to the ACC remaining in the material is centered at 168.6 ppm, while three additional signals centered at 170.6 ppm, 169.5 ppm, and 168.7 ppm are assigned to two ^{13}C atomic sites in vaterite and the single ^{13}C atomic environment present in calcite, respectively. The narrow linewidths for the vaterite and calcite signals (0.5 ppm fwhm, 0.7 ppm fwhm, and 0.4 ppm fwhm, respectively) are indicative of a uniform local atomic order for each of the sites, while the broadened linewidth for the remaining ACC (3.2 ppm fwhm) reveals that the sample was not fully crystalline. The relative amounts of the distinct ^{13}C sites are quantified by integration of the applied Lorentzian line fits (Table 3). After 48 hours at 76% relative humidity, the calcium carbonate material prepared with a sucrose surface additive was composed of 37% of the first crystallographic site attributed to vaterite, 16% of the second crystallographic site attributed to vaterite, 13% of the single crystallographic site attributed to calcite, and 34% of the distribution of sites assigned to amorphous calcium carbonate. As with the vaterite present in the samples prepared without surface additive and with a glucose surface additive, the vaterite sites occur in a 2:1 ratio given the error present in the fitting. The corresponding single-pulse ^{1}H measurements reveal that two distinct ^{1}H atomic environments are still present in the material; the broadened ^{1}H signal centered at 5.0 ppm (4 ppm fwhm) indicates that a significant amount of structural water remained associated with the ACC in the material after 48 hours of crystallization while the ^{1}H signal centered at 1.3 ppm (2 ppm fwhm) indicates that structural hydroxyl groups were present in the amorphous calcium carbonate, with additional intensity resulting from sucrose hydroxyl groups that were

present in the carbonate material. The linewidth of the structural water signal has decreased slightly and the intensity has correspondingly increased, which is consistent with the increased atomic order present in the material. In summary, after 48 hours at 76% relative humidity, vaterite and calcite crystals began to nucleate and grow in the amorphous calcium carbonate nanoparticles prepared with a sucrose adsorbate although a significant amount of amorphous material remained. In addition, the amorphous calcium carbonate nanoparticles crystallized preferentially to the metastable vaterite polymorph in the presence of a sucrose (non-reducing saccharide) surface additive, although some of the thermodynamically stable calcite polymorph was also present. Interestingly, the amorphous calcium carbonate nanoparticles crystallized in the presence of a glucose (reducing saccharide) surface additive for 48 hours exhibited significantly larger amounts of amorphous material (98% relative abundance) in comparison with those crystallized in the presence of a sucrose surface additive (34% relative abundance), indicating that sucrose delayed the onset of crystallization, but to a lesser extent than glucose.

After exposure to 76% relative humidity for 120 hours (Figure 17, 120 hours), the XRD pattern obtained for the calcium carbonate material prepared with a sucrose surface additive exhibits two sets of narrow reflections that are indexable to vaterite and calcite. The intensities of the reflections indicate that the material was fully crystalline and vaterite reflections still have greater intensity in comparison to the calcite reflections, confirming that there was a larger amount of metastable vaterite relative to calcite in the material. Correspondingly, the single-pulse ^{13}C NMR measurements establish that crystalline vaterite and calcite were present in the material and no amorphous calcium carbonate remained. Signals at 170.6 ppm, 169.5 ppm, and 168.7 ppm assigned to the two ^{13}C atomic sites in

vaterite and the single ^{13}C atomic environment present in calcite, respectively, have narrow linewidths (0.5 ppm fwhm, 0.7 ppm fwhm, and 0.4 ppm fwhm, respectively) which are indicative of a uniform local atomic order consistent with a fully crystalline material. The integration of the deconvoluted signals establishes that the material was composed of 61% of the first ^{13}C atomic environment attributed to vaterite, 26% of the second ^{13}C atomic environment attributed to vaterite, and 13% of the ^{13}C atomic environment attributed to calcite. Again, it is notable that within a few percent error of the fitting, the relative populations of the crystallographic sites attributed to vaterite occurred in a 2:1 ratio. The ^{1}H NMR measurements also confirm that the calcium carbonate material had become more ordered. The ^{1}H signal centered at 1.3 ppm associated with the structural -OH groups in the amorphous material and potentially with the -OH groups present in the sucrose surface additive has decreased in intensity, consistent with the crystallization of the amorphous material. Furthermore, the ^{1}H signal corresponding to the structural water has shifted from 5.0 ppm to 4.8 ppm and narrowed considerably (2 ppm fwhm), indicating that the water associated with the crystalline material had a more uniform atomic environment as expected. As previously discussed, the signal shift is likely due to the exclusion of structural water from the carbonate material as it crystallized, leaving only surface water. Altogether, the XRD and solid-state NMR measurements establish that after 120 hours at 76% relative humidity, no amorphous calcium carbonate remained in the calcium carbonate nanoparticles synthesized with a sucrose surface additive.

To summarize the significant findings from this series of XRD and solid-state NMR measurements, the amorphous calcium carbonate material crystallized in the presence of a sucrose (non-reducing saccharide) surface additive had a delayed onset of crystallization in

comparison with the same ACC crystallized without a surface additive. Crystallization was first manifested to a significant extent after 48 hours at 76% relative humidity in the presence of the sucrose surface additive, in comparison to 8 hours without any surface additive present. Although both the sucrose and glucose saccharide surface additives delayed the onset of crystallization, crystallization did take place more rapidly in the presence of the sucrose surface additive than in the presence of the glucose (reducing saccharide) surface additive. After 48 hours at 76% relative humidity, the material with a sucrose surface additive was composed of 34% ACC, while the material prepared with a glucose surface additive contained 98% ACC. Furthermore, although the thermodynamically stable calcite polymorph predominated in the fully crystalline calcium carbonate material with a glucose surface additive (67% relative abundance) and in the crystalline calcium carbonate prepared without surface additives (90% relative abundance), it was present in significantly lower levels in the sample crystallized with a sucrose surface additive (13% relative abundance). The kinetically metastable vaterite was the predominant polymorph produced in the presence of sucrose (87% relative abundance) versus in the presence of glucose (33% relative abundance) and no surface additive (10% relative abundance). In conclusion, the sucrose surface additive delayed the onset of crystallization in amorphous calcium carbonate (although to a lesser extent than glucose), as well as favored the formation of metastable vaterite over the thermodynamically stable calcite.

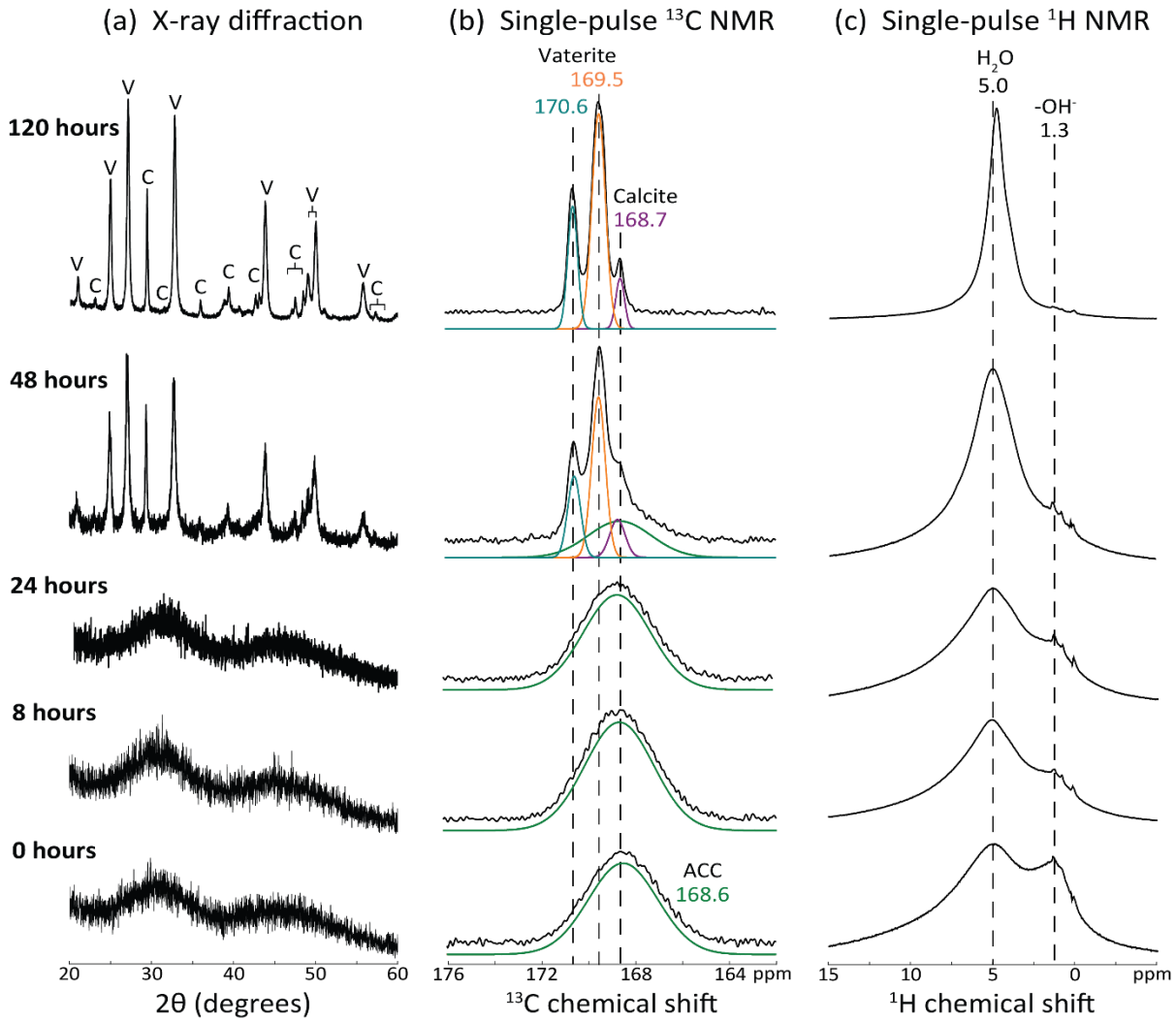

Figure 17. (a) Wide-angle powder XRD patterns, (b) solid-state single-pulse ^{13}C NMR spectra, and (c) solid-state single-pulse ^{1}H NMR spectra were acquired for amorphous calcium carbonate synthesized with a sucrose surface additive and crystallized at 76% relative humidity for 0, 8, 24, 48, and 120 hours. XRD reflections were indexed to standard calcite (C) and vaterite (V) reflections. NMR spectra were acquired at 9.4 T, 298 K, and 10 kHz MAS and chemical shifts were referenced using a tetrakis(trimethylsilyl)silane (TKS) standard. Lorentzian line fits were applied to the ^{13}C NMR spectra to deconvolute the overlapping signals and quantify the relative amounts of each calcium carbonate polymorph.

Crystallization time (hrs)	Amorphous $CaCO_3$	Calcite	Vaterite Site 1	Vaterite Site 2
0	100%	-	-	-
8	100%	-	-	-
24	100%	-	-	-
48	34%	13%	37%	16%
120	-	13%	61%	26%

Table 3. Relative quantities of calcium carbonate polymorphs present in the calcium carbonate material prepared with a sucrose surface additive and stored at 76% relative humidity for 0, 8, 24, 48, and 120 hours. Quantities are obtained from integration of Lorentzian line fits applied to solid-state single-pulse ^{13}C NMR spectra.

Complementary solid-state ^{13}C CP-MAS NMR measurements were performed on the same calcium carbonate material prepared with a sucrose adsorbate using 500 ms and 3750 ms contact times to characterize the ^{13}C atomic sites in different molecular proximities to ^{1}H atomic sites. The initial measurements (Figure 18, 0 hours) obtained with a 500 ms contact time contain a single inhomogeneously broadened signal (3.4 ppm fwhm) centered at 168.6 ppm indicating that a wide distribution of ^{13}C atomic sites are adjacent to ^{1}H atomic sites. As in the previous CP-MAS NMR measurements, the signal intensity results primarily from protons in structural water and hydroxyl groups found throughout the highly disordered ACC that are in close molecular proximity to the carbonate anions, while the chemical shift is consistent with the average chemical shift assigned to the ^{13}C environments in amorphous calcium carbonate. The observed signal also contains intensity resulting from the protons within the saccharide molecules that are proximate to surface carbonate species. As expected, increasing the contact time from 500 ms to 3750 ms contact time increases the signal to noise ratio, however the chemical shift of the signal (168.6 ppm) and the signal width (3.4 ppm fwhm) remain the same. The increased contact time allows for the detection of a larger number of ^{13}C atomic sites in the material as spin polarization travels radially outward from

the ^{1}H nuclei for a longer amount of time, thus increasing the signal to noise ratio. The identical chemical shifts and line widths for the 500 ms and 3750 ms contact times indicate that the ^{13}C atomic sites adjacent to the ^{1}H atomic sites had a similar average electronic shielding as well as distribution at different molecular proximities. Furthermore, the signals for the 500 ms and 3750 ms contact time are unchanged across a 24 hour time period (Figure 18, 0 hours, 8 hours, 24 hours), signifying that the structural water and -OH groups associated with amorphous calcium carbonate and sucrose surface additive remained in the material and the molecular proximities of the ^{1}H and ^{13}C nuclei and distributions of ^{13}C atomic environments both remained the same.

After the calcium carbonate material prepared with a sucrose surface additive was exposed to 76% relative humidity for 48 hours, the obtained ^{13}C CP-MAS NMR measurements differ slightly from those obtained for the first three timepoints (Figure 18, 48 hours). The peak intensities and linewidths for both the 500 ms contact time (3.0 ppm fwhm) and the 3750 ms contact time (3.2 ppm fwhm) have decreased and the centers of the signals have shifted to 168.9 ppm. The decrease in linewidth indicates that the molecular environments for the ^{13}C nuclei proximate to the ^{1}H nuclei had a more uniform order and the signal shift corresponds to an average ^{13}C atomic environment that between that of calcite and that of vaterite. In addition, the observed decrease in signal intensity results from the exclusion of the structural water and -OH groups associated with the disordered amorphous material; any remaining water was likely physisorbed to the calcite and vaterite crystallites at the particle surface. Notably, the shift in the average ^{13}C atomic environment was not observed for the calcium carbonate material crystallized without surface additive present, which could indicate that once the structural water and hydroxyl groups in the carbonate

material were depleted by crystallization, a larger portion of the CP signal resulted from the protons on saccharide molecules that were adjacent to carbonate anions at the particle surface. The saccharide molecules were likely associated with a more metastable phase of calcium carbonate, such as vaterite, which could result in the observed signal shift. Finally, the signal shift and linewidth are similar for the 500 ms and 3750 ms contact times, establishing that the ^{13}C environments that were adjacent to the ^{1}H nuclei were uniformly distributed across a range of distances.

Similarly, after 120 hours at 76% relative humidity, the single signal observed in the ^{13}C CP-MAS NMR measurements at contact times of 500 ms and 3750 ms has decreased further in intensity and linewidth (2.0 ppm), and shifted to 169.3 ppm. These changes result from the increased crystallinity present in the sample as described previously. It is interesting to note that the signals now correspond well with the known chemical shift of the first vaterite site (169.5 ppm), indicating that the protons that remained in the calcium carbonate material prepared with a sucrose adsorbate were proximate to vaterite sites. The identical shift and linewidth for the two contact times again indicates that the ^{13}C environments that were adjacent to the ^{1}H nuclei were uniformly distributed across a range of distances.

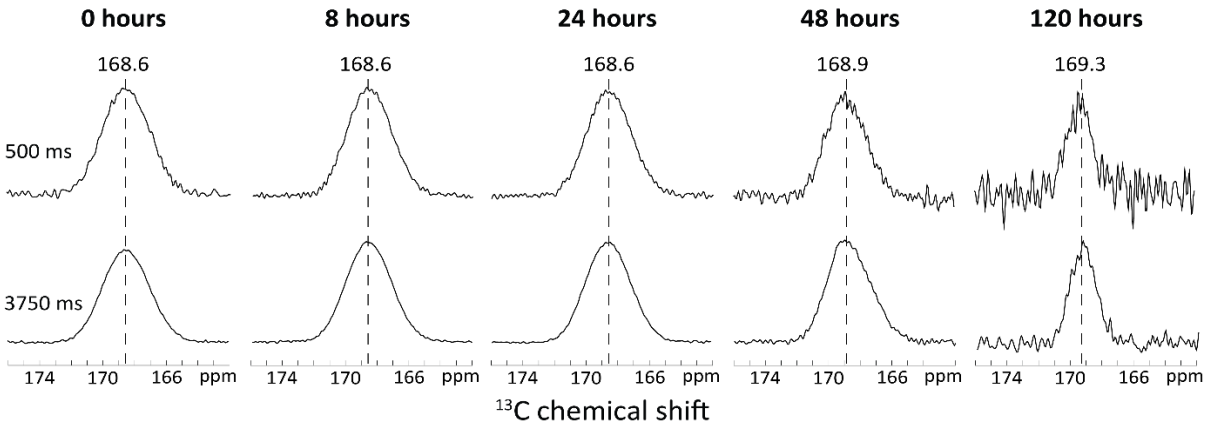

Figure 18. Solid-state ^{13}C CP-MAS NMR spectra were acquired for the same amorphous calcium carbonate synthesized with a sucrose surface additive and crystallized at 76% relative humidity for 0, 8, 24, 48, and 120 hours as in Figure 17. NMR spectra were acquired for contact times of 500 ms and 3750 ms at 9.4 T, 298 K, and 10 kHz MAS and referenced using a tetrakis(trimethylsilyl)silane (TKS) standard.

To further characterize the fully crystalline calcium carbonate material prepared with a sucrose surface additive (120 hours at 76% relative humidity), separate solid-state single-pulse ^{43}Ca measurements were conducted at the National High Magnetic Field Laboratory (Figure 19). Two distinct signals are resolved in the ^{43}Ca measurements by deconvolution using Lorentzian line fits, indicating that two distinct ^{43}Ca environments are present in the material. The narrow (5 ppm fwhm) signal centered at 19 ppm is attributed to the single ^{43}Ca environment present in calcite, while the broadened signal (20 ppm fwhm) centered at 5 ppm corresponds to the average ^{43}Ca environment present in vaterite. Both polymorphs of calcium carbonate are expected in the material based on the separate solid-state single-pulse ^{13}C measurements and wide-angle XRD measurements conducted on a sample prepared and crystallized under the same conditions. As observed in the previous ^{43}Ca measurements, there is only one broadened ^{43}Ca signal attributed to vaterite although the ^{13}C measurements reveal that crystalline vaterite has two distinct ^{13}C sites with relatively uniform distributions (0.5 ppm and 0.7 ppm fwhm). Again, it is likely that the single broadened ^{43}Ca vaterite signal is

composed of multiple overlapping signals resulting from ^{43}Ca sites which have similar average electronic shielding. Integrating the deconvolutions reveals that the calcium carbonate material crystallized in the presence of a sucrose surface additive was composed of 23% of the single ^{43}Ca site attributed to calcite and 77% of the distribution of ^{43}Ca sites attributed to vaterite. In comparison, the relative populations indicated by the single-pulse ^{13}C NMR measurements (Figure 17, 120 hours) were 13% of the single ^{13}C site assigned to calcite and 87% of the two ^{13}C sites assigned to vaterite (Table 3). Again, the differences observed between the two samples prepared and crystallized under identical conditions may be attributed to the fact that the crystallization of metastable calcium carbonate is inherently difficult to control, and agreement within +/- 10% of the relative abundance of the crystalline polymorphs present is adequate.

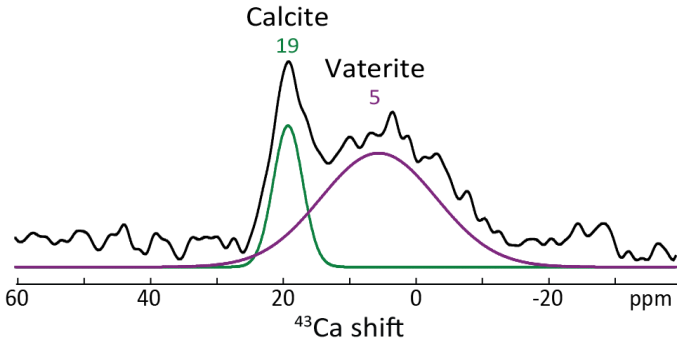

Figure 19. Solid-state single-pulse ^{43}Ca MAS NMR spectrum was acquired for amorphous calcium carbonate synthesized with a sucrose surface additive and crystallized at 76% relative humidity for 120 hours. NMR spectrum was acquired at 11.7 T, 298 K, and 5 kHz MAS and referenced using a 1.0 M $CaCl_2$ standard solution.

Particle morphology and crystallinity were characterized using complementary SEM, TEM, and BET measurements conducted on a calcium carbonate material prepared with a sucrose adsorbate and crystallized under the same conditions (Figure 20). Measurements were obtained before (0 hours at 76% relative humidity) and after (120 hours at 76% relative humidity) crystallization. Aggregates of spherical nanoparticles averaging 100 nm in

diameter are visible in the SEM images obtained for both the amorphous material (0 hours) and the crystalline material (120 hours), showing that the morphology and particle diameter did not change significantly as a result of the crystallization process (Figure 20a). Similarly, the bright-field TEM measurements obtained before and after the crystallization of the calcium carbonate material reveal that the particles were roughly spherical with an average diameter of 100 nm (Figure 20b). As with the sample crystallized in the presence of glucose, the increased particle roughness observed for the amorphous calcium carbonate crystallized without surface additive is not observed. This potentially results from the retention of larger amounts of structural water in the calcium carbonate particles, as sucrose serves as a cryoprotectant. BET analysis reveals that the initial surface area of the calcium carbonate material with a sucrose adsorbate was 35.3 ± 0.3 m^2/g while the surface area after crystallization is complete was around 24.7 ± 0.2 m^2/g, which are similar to the surface areas measured for the calcium carbonate material prepared and crystallized with a glucose surface additive. The observed decrease in surface area was likely caused by particle densification associated with the crystallization of an amorphous material. Again, these surface areas are noticeably higher than those measured for the amorphous material crystallized without surface additives, which could be the result of the sucrose surface additive inhibiting particle aggregation during synthesis. The corresponding electron diffraction patterns for the bright-field TEM images (Figure 20c) indicate that the calcium carbonate material as synthesized was completely amorphous, while the pattern collected after the calcium carbonate material was stored at 76% relative humidity for 120 hours exhibits regular scattering characteristic of a polycrystalline material with some large single crystals. The dark-field TEM (Figure 20d)

supports these observations, as numerous small crystallites of a few nanometers in width are visible alongside several crystalline regions that are much larger in size (10-50 nm).

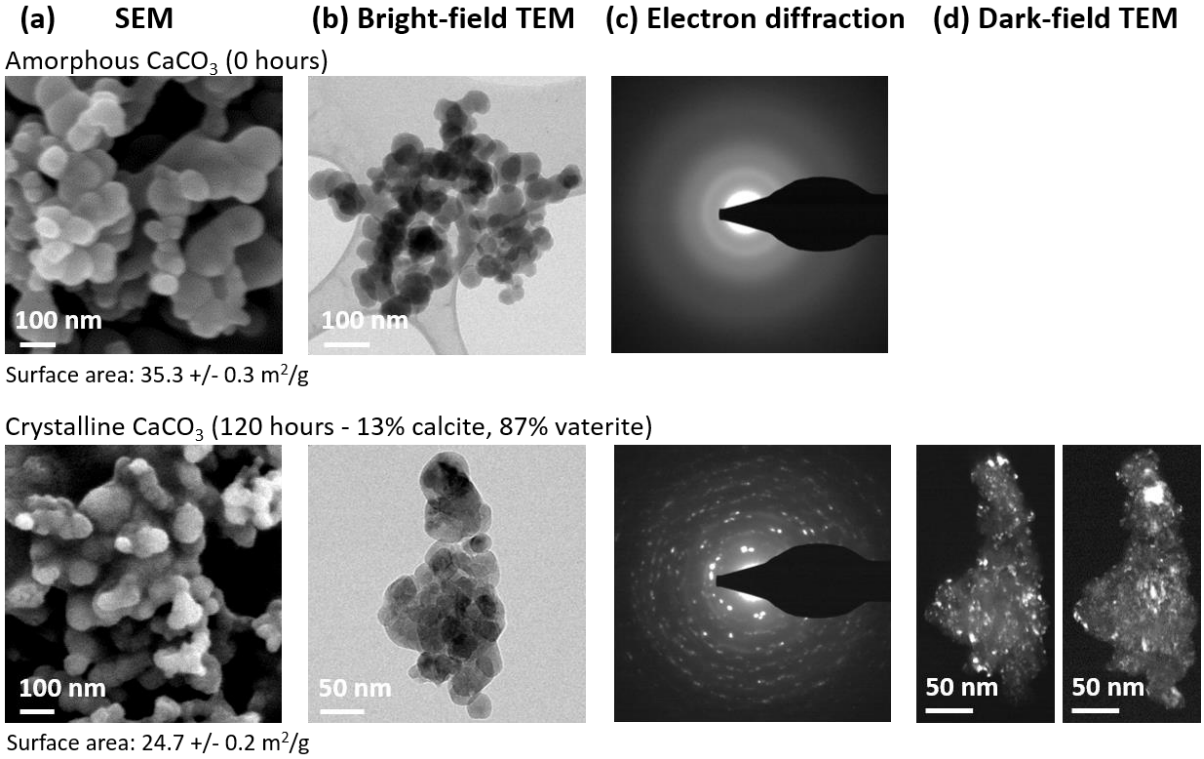

Figure 20. (a) Scanning electron micrographs, (b) bright-field transmission electron micrographs, (c) selected area electron diffraction patterns, and (d) dark-field transmission electron micrograph acquired for amorphous calcium carbonate synthesized with a sucrose surface additive and crystallized at 76% relative humidity for 0 and 120 hours. Compositions are based upon single-pulse ^{13}C NMR measurements conducted on a sample prepared and crystallized under the same conditions (Figure 17 and Table 3). A dark-field TEM image was not collected at 0 hours as the material was diffracting electrons at random, therefore the dark-field image did not exhibit any contrast.

A 2D $^{13}C\{^{1}H\}$ HETCOR NMR spectrum was acquired for amorphous calcium carbonate synthesized with a sucrose surface additive and crystallized at 76% relative humidity for 120 hours (Figure 21a). A strong intensity correlation is measured between the average carbonate environment (169.3 ppm) and water (4.8 ppm), while a weaker correlation is measured between the average carbonate environment and hydroxyl groups (0 ppm). The first correlation is consistent with water that was excluded from the fully crystalline calcium

carbonate material and is adsorbed to the surface of the particles (Figure 21b). The second weaker correlation is potentially consistent with interactions between the hydroxyl groups remaining within the calcium carbonate material and the carbonate anions present within the carbonate material, or close molecular proximity of the saccharide hydroxyl groups with surface carbonate species (Figure 21b). It is notable that no correlations are present farther downfield in the proton dimension that would signify hydrogen bonding between the saccharide additive and the carbonate anion. The interactions of the sucrose surface additive with the carbonate anion could benefit from characterization by dynamic nuclear polarization-enhanced NMR, which is sensitive to surface species and interactions.

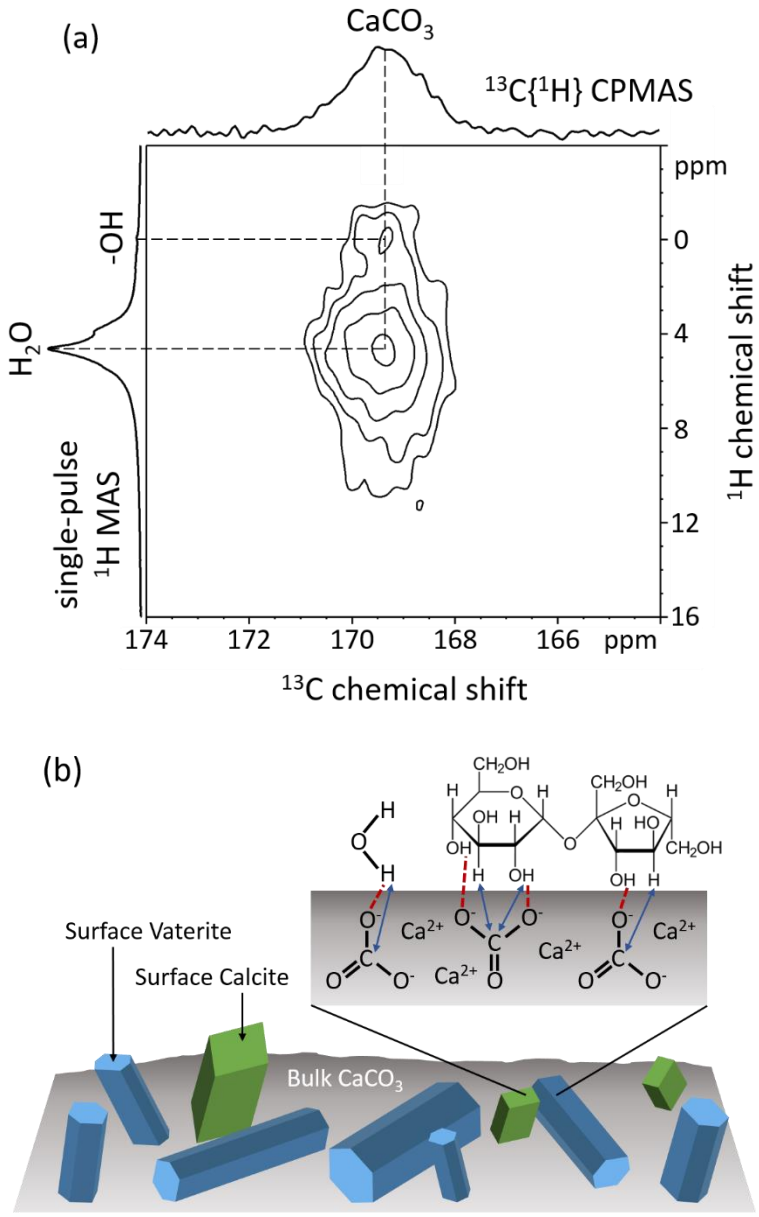

Figure 21. (a) Solid-state 2D $^{13}C\{^{1}H\}$ HETCOR NMR spectrum acquired for amorphous calcium carbonate synthesized with a sucrose surface additive and crystallized at 76% relative humidity for 120 hours. 1D ^{13}C CP-MAS and single-pulse ^{1}H MAS spectra displayed along the horizontal and vertical axes, respectively. (b) Depiction of the interaction of sucrose (non-reducing saccharide) with the crystal structures present at the calcium carbonate particle surface.

3.2.3. Other reducing and non-reducing saccharides

Additional wide-angle powder XRD measurements were collected for calcium carbonate synthesized and crystallized in the presence of other reducing (maltose) and non-reducing (trehalose) saccharide adsorbates in addition to the original reducing (glucose) and non-reducing (sucrose) saccharide adsorbates. These measurements were performed to further examine the effects of saccharide stereochemistry on the crystallization process of amorphous calcium carbonate. All of the calcium carbonate materials were fully amorphous after synthesis based on the broad, low intensity reflections centered at 30° and 45° 2θ indicative of random scattering of the x-rays (Figure 22, 0 hours).

The crystallization process of the material synthesized without surface additive was nearly identical to that observed previously; crystallization was completed by 24 hours at 76% relative humidity and calcite was the predominant polymorph present in the sample (Figure 22, No additive, 24 hours). Although some vaterite was observed in the previous sample based on XRD and single-pulse ^{13}C NMR measurements, there was no vaterite present in this sample based on XRD measurements. The differences observed between the two samples prepared and crystallized under identical conditions may be attributed to the fact that the crystallization of metastable calcium carbonate is inherently difficult to control, and agreement within +/- 10% of the relative abundance of the crystalline polymorphs present is adequate.

Additionally, the crystallization process of the material synthesized with a sucrose surface adsorbate was similar to that observed previously; crystallization was initiated between 24 and 48 hours at 76% relative humidity and completed by 72 hours at 76% relative humidity (Figure 22, Sucrose, 48 hours and 72 hours). In comparison, the XRD and

single-pulse ^{13}C NMR measurements conducted on the first sample indicated that crystallization was initiated between 24 and 48 hours and completed by 120 hours, as a 72 hour time point was not taken (Figure 17, 48 hours and 120 hours). Vaterite was the predominant polymorph in the material based on the XRD measurements with trace amounts of calcite present, which is consistent with the measurements obtained for the first sample as well. It is notable that the XRD measurements obtained at 72 hours and 240 hours are nearly identical (Figure 22, Sucrose, 72 hours and 240 hours), indicating that vaterite remained the predominant polymorph in the material after 10 days at 76% relative humidity and that the metastable vaterite phase was kinetically stabilized by the sucrose adsorbate for extended periods of time.

Furthermore, the XRD measurements for the material synthesized with a glucose surface additive reveal that crystallization was initiated at 48 hours and completed by 240 hours at 76% relative humidity (Figure 22, Glucose, 48 hours and 240 hours). These measurements are consistent with the XRD and single-pulse ^{13}C NMR measurements obtained for the first sample, with crystallization initiated at 48 hours and completed by 120 hours, as the 120 hour time point was taken in place of the 240 hour time point (Figure 12, 48 hours and 120 hours). The additional measurement performed after 72 hours at 76% relative humidity reveals that the sample was almost completely amorphous (Figure 22, 72 hours), which indicates that the progression of the crystallization process was slowed by the presence of a glucose surface additive. Calcite was the predominant polymorph in the material with some vaterite present, which is again consistent with the XRD and single-pulse ^{13}C NMR measurements obtained for the first sample. The vaterite remained in the sample after 240 hours at 76% relative humidity, signifying that it was stabilized by the presence of a glucose surface additive.

The XRD measurements conducted on the amorphous calcium carbonate synthesized with a trehalose surface additive exhibit distinct differences from those obtained for the sucrose surface additive. Although both saccharides are non-reducing, crystallization was initiated at 24 hours and completed by 48 hours in the material synthesized with a trehalose surface additive, in comparison with the 48 hours and 72 hours, respectively, observed for sucrose (Figure 22, 24 hours, 48 hours, 72 hours). Furthermore, the material crystallized in the presence of trehalose contained mostly calcite based on XRD measurements, with only trace amounts of vaterite present. In comparison, the sucrose adsorbate favored the formation of vaterite, with only trace amounts of calcite formed. The differences in the crystallization processes and the formation of the different polymorphs were likely a result of the differences in stereochemistry and bond lengths exhibited by the two non-reducing saccharides. Trehalose is a disaccharide composed of two glucose molecules joined by an α-β (1-1) glycosidic bond, while sucrose is a disaccharide composed of a glucose and fructose molecule joined by an α-β (1-2) glycosidic bond.

Similarly, the XRD measurements conducted on the amorphous calcium carbonate synthesized with a maltose surface additive exhibit distinct differences from those obtained for the glucose surface additive. Although maltose and glucose are both reducing saccharides, crystallization was initiated at some point between 72 and 240 hours and was complete by 240 hours in the material synthesized with a maltose surface additive, compared to the 48 hours and 72 hours, respectively, observed for glucose (Figure 22, Maltose, 72 hours and 240 hours and Glucose, 48 hours and 72 hours). Additionally, the material crystallized in the presence of maltose contained primarily calcite based on XRD measurements, with only small amounts of vaterite present, which is consistent with the

polymorphs resulting from the crystallization of amorphous calcium carbonate with a glucose surface additive. Again, the differences in the delay of the onset of crystallization were likely a result of the differences in stereochemistry and bond lengths exhibited by the two reducing saccharides. Maltose is a disaccharide composed of two glucose molecules joined by an α-α (1-4) glycosidic bond, while glucose is a monosaccharide.

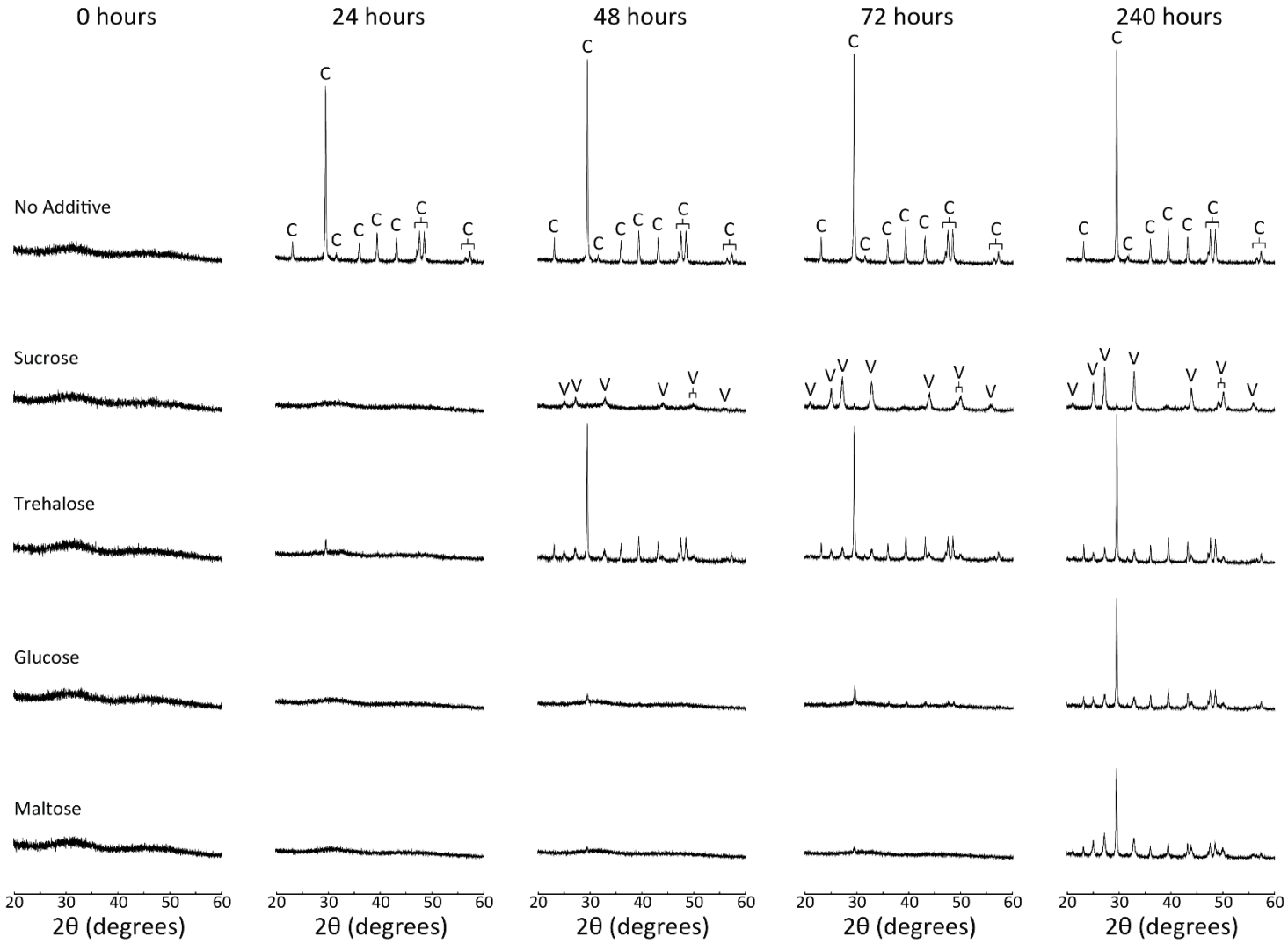

Figure 22. Wide-angle powder XRD patterns were acquired for amorphous calcium carbonate synthesized without surface additive and with sucrose, trehalose, glucose, and maltose surface additives and crystallized at 76% relative humidity for 0, 24, 48, 72, and 240 hours. XRD reflections were indexed to standard calcite (C) and vaterite (V) reflections.

4. Conclusions and future work

4.1. Conclusions

Based on the x-ray diffraction, nuclear magnetic resonance, electron microscopy, and nitrogen adsorption measurements presented previously, this work has shown that saccharides adsorbed on amorphous calcium carbonate nanoparticles delay the onset and progression of crystallization. The efficacy with which the saccharides delay the crystallization process and the polymorphs of calcium carbonate that result from the crystallization process vary based upon the stereochemistry of the saccharides. In the absence of surface additives, neat amorphous calcium carbonate nanoparticles began to crystallize after 8 hours of exposure to 76% relative humidity. The crystallization process was completed by 24 hours, and the predominant polymorph formed was the thermodynamically stable calcite polymorph (90% relative abundance), with trace amounts of the metastable vaterite polymorph present (10% relative abundance).

When amorphous calcium carbonate nanoparticles were synthesized in the presence of glucose, a reducing saccharide, the onset of crystallization was delayed by up to 40 hours, and the crystallization process was completed by 120 hours. Data acquired at intermediate times indicated that the progression of crystallization was slowed as well, as the material was primarily amorphous after 72 hours of exposure to 76% relative humidity. Although the calcite polymorph still predominated (67% relative abundance) in the fully crystalline material, there was significantly more vaterite present (33% relative abundance) compared to the neat ACC synthesized and crystallized without adsorbed saccharides. The delay in the onset of the crystallization process and the formation and stabilization of larger amounts of vaterite potentially resulted from electrostatic interactions of surface Ca^{2+} species with

deprotonated glucose hydroxyl groups, or from hydrogen bonding of surface CO_3^{2-} species with glucose hydroxyl groups.

When the amorphous calcium carbonate nanoparticles were synthesized with a sucrose (non-reducing disaccharide) adsorbate, the onset of crystallization was delayed by slightly less than 40 hours, and the crystallization process was completed by 120 hours. In contrast to the materials synthesized with no additive and with a glucose surface additive, the calcium carbonate synthesized with a sucrose surface additive crystallized selectively to vaterite (87% relative abundance), with small amounts of calcite present (13% relative abundance). Remarkably, the vaterite appeared to be stable as the material remained unchanged after storage at 76% relative humidity for 10 days (see Figure 22). As before, the delay in the onset of the crystallization process and the formation and stabilization of significant amounts of stable vaterite potentially resulted from electrostatic interactions of surface Ca^{2+} species with deprotonated sucrose hydroxyl groups, or from hydrogen bonding of surface CO_3^{2-} species with sucrose hydroxyl groups. Interestingly, the formation of the crystalline calcium carbonate polymorphs in the bulk material was strongly affected by the presence of a sucrose surface additive. This is indicated by the selective formation of bulk vaterite, suggesting that the crystallization of amorphous calcium carbonate was initiated at the particle surface and progressed inward. Additionally, the extended stability of the vaterite was likely a result of sucrose adsorbate interactions that restricted water access to the vaterite surfaces and thereby inhibited the nucleation of other carbonate polymorphs. Although it could be argued that simply slowing the kinetics of the crystallization process with a surface additive would induce the formation of a larger amount of the metastable vaterite polymorph, the glucose surface additive delayed the onset and progression of the crystallization process to a larger

extent and significant amounts of calcite were still formed. The differences exhibited by the two saccharides in inhibiting crystallization and stabilizing different calcium carbonate polymorphs may be attributed to the architectural differences of the respective saccharides, which affect interactions with the particle surface. Glucose is a reducing monosaccharide which ring-opens at high pH to form a saccharinic acid with carboxylate groups. The carboxylate groups potentially interact with the calcium carbonate particles via electrostatic interactions. In contrast, sucrose is a non-reducing disaccharide composed of glucose and fructose monomers which does not ring-open at high pH and likely exhibits both hydrogen bonding and electrostatic interactions. Similarly, glucose and sucrose inhibit hydration of aluminosilicate cement materials to different extents, and this phenomenon has been definitively correlated with architectural variances.[32,39]

Preliminary extension of the experiments to two reducing (maltose - a disaccharide composed of two glucose monomers linked by an α-α (1-4) glycosidic bond) and non-reducing (trehalose - a disaccharide composed of two glucose monomers linked by an α-β (1-1) glycosidic bond) saccharides yielded informative results with regards to crystalline polymorph formation based on saccharide stereochemistry. Both surface additives delayed the onset of crystallization, trehalose by up to 16 hours and maltose by more than 64 hours and the crystallization process was complete in the two materials by 48 hours and 240 hours, respectively. The crystalline calcium carbonate products both contained significant amounts of calcite with some vaterite present, indicating that saccharide stereochemistry has a significant role in the stabilization of the metastable vaterite polymorph, as neither saccharide favored the formation of vaterite to the extent that sucrose did.

In summary, the results of these studies demonstrated the importance of saccharide stereochemistry in inhibiting and controlling the crystallization process of amorphous calcium carbonate nanoparticles. Application of this directed crystallization will allow for specific stabilization of promising metastable polymorphs, such as vaterite, and subsequent use in various technological applications including drug delivery. Further research into the specific surface additive interactions and their impact on the resultant crystalline polymorphs will allow for the intelligent selection of surface additives and enable the successful conversion of CO_2 waste into useful products.

4.2. Future work

While the work in this thesis extensively details the effects of saccharide surface additives on the transient crystallization processes of metastable calcium carbonate, several experiments should be performed to augment it. Although it was not mentioned in the thesis, the amounts of saccharide surface additive were determined indirectly by performing solution-state ^{1}H NMR measurements on the synthesis filtrate to quantify the amounts of unabsorbed saccharide, however the results are in direct contradiction with the TEM, SEM, and ^{1}H NMR measurements. The saccharide surface additives were both determined to be present in a 1:1 ratio by weight of sample, which based upon the absence of a large signal in the ^{1}H NMR resulting from the sugar protons (by comparison, water is present at 10% bwos based upon TGA measurements), is unlikely. Furthermore, the particle sizes based on the SEM and TEM measurements did not change between the calcium carbonate synthesized without and with saccharide surface additive, which should not be the case if the saccharide were present in a 1:1 ratio. Additionally, the TEM images do not indicate that a noticeable surface additive layer is present, as they have in other works utilizing a significant amount of

surface additive.[40] It is suggested that the amount of saccharide surface additive be determined directly by dissolving a known amount of calcium carbonate prepared with surface additive in strong acid, then bringing the solution to a neutral pH with base and measuring the saccharide concentration using solution-state NMR. Additionally, a solid-state 2D $^{13}C\{^{1}H\}$ HETCOR NMR spectrum could be acquired for amorphous calcium carbonate synthesized with a glucose surface additive and crystallized at 76% relative humidity for 120 hours.

Furthermore, additional techniques should be used to characterize the interactions between saccharides and the calcium carbonate particle surface and also to study the crystallization processes of metastable calcium carbonate synthesized with and without surface additives. Dynamic nuclear polarization-enhanced NMR (DNP) could provide further insights into the interactions of the saccharide additives with the ACC particle surfaces as it affords several key advantages over traditional NMR measurements. DNP employs polarization transfer from electrons to the nuclei of interest, and the increased sensitivity of electrons to polarization results in significant signal enhancements. Additionally, DNP is a surface sensitive technique ideal for characterizing surface additive interactions as the polarized electrons transfer from radicals in solution to the sample surface. The surface forces apparatus (SFA) could also yield insights into the types and strengths of the interactions between the amorphous calcium carbonate particles and the saccharide surface additives utilizing recently developed ACC surfaces brought into contact under relevant solution conditions. Additionally, electron tomography could potentially be used to further characterize the crystallization processes of the calcium carbonate materials, specifically providing insights into where the crystallization process is initiated in the particles prepared

with and without surface additives and how the crystallization process progresses with time. These measurements were attempted, but due to the instabilities of the material under the electron beam, accurate characterization presented challenges. Finally, gas pycnometry could be utilized to characterize the densification of the carbonate materials as crystallization progresses, as amorphous materials are known to be less dense than crystalline materials, and these results could be compared with the extents of crystallization as determined using NMR.

Additionally, inspiration for additional surface additives should be taken from the adhesion of mussels to rocks in the presence of seawater using specialized mussel foot proteins. It has been demonstrated that the process depends on a synergy between electrostatic interactions, which break the hydration layer present at the mineral-water interface, and hydrogen bonding, which allows the molecules to strongly adsorb to the mineral surface.[41] Neither electrostatic interactions nor hydrogen bonding alone exhibit as strong of an adsorption. The stabilization of amorphous calcium carbonate in marine environments could depend on a similar synergy between electrostatic interactions and hydrogen bonding, with the amino acids found in proteins and the saccharides found in chitosan and chitin allowing for stronger adsorption and stabilization of ACC than either would alone. Preliminary research has already been conducted regarding the stabilization of amorphous calcium carbonate by mussel foot protein inspired molecules, although the interactions of the molecules with the ACC were not well characterized.[40] Furthermore, the use of a reducing saccharide (glucose) in conjunction with a non-reducing saccharide (sucrose) could provide the same combination of electrostatic and hydrogen bonding interactions with the ACC particle surface, stabilizing the ACC more efficaciously than either did alone.

Finally, as shown in the SEM and TEM images acquired before and after crystallization, the spherical amorphous calcium carbonate nanoparticles crystallize to form spherical polycrystalline nanoparticles containing vaterite and calcite crystallites. As the solid-state transformation of ACC to crystalline polymorphs does not alter particle morphologies, ACC should be crystallized in solution to influence the particle morphologies and aspect ratios resulting from the crystallization process. Work has been performed studying the crystallization of amorphous calcium carbonate using templated growth in track etch membranes to form high-aspect ratio calcite nanorods,[17] and by adjusting the solution conditions and additives it is probable the polymorph may be changed to either aragonite or vaterite as well. Regarding the synthesis of the aragonite polymorph from amorphous calcium carbonate, it has been demonstrated in the literature that aragonite will form from an ACC precursor in the presence of magnesium ions.[42] In preliminary experiments not detailed in this thesis, structural strontium or barium in the amorphous calcium carbonate particles will result in the formation of aragonite as the ACC crystallizes. Both strontium carbonate and barium carbonate are isostructural with aragonite, exhibiting the same orthorhombic *Pmcn* space group, therefore strontium and barium ions stabilize the formation of the aragonite polymorph over calcite or vaterite.

5. References

1. Variankaval, N., Cote, A. S. & Doherty, M. F. "From form to function: Crystallization of active pharmaceutical ingredients." *AIChE J.* **54,** 1682–1688 (2008).
2. Chen, J., Sarma, B., Evans, J. M. B. & Myerson, A. S. "Pharmaceutical Crystallization." *Cryst. Growth Des.* **11,** 887–895 (2011).
3. Shekunov, B. Y. & York, P. "Crystallization processes in pharmaceutical technology and drug delivery design." *J. Cryst. Growth* **211,** 122–136 (2000).
4. Epping, J. D. & Chmelka, B. F. "Nucleation and growth of zeolites and inorganic mesoporous solids: Molecular insights from magnetic resonance spectroscopy." *Curr. Opin. Colloid Interface Sci.* **11,** 81–117 (2006).
5. Messinger, R. J., Na, K., Seo, Y., Ryoo, R. & Chmelka, B. F. "Co-development of Crystalline and Mesoscopic Order in Mesostructured Zeolite Nanosheets." *Angew. Chem. Int. Ed. Engl.* **54,** 927–31 (2015).
6. Na, K., Jo, C., Kim, J., Cho, K., Jung, J., Seo, Y., Messinger, R. J., Chmelka, B. F. & Ryoo, R. "Directing Zeolite Structures into Hierarchically Nanoporous Architectures." *Science* **333,** 328–332 (2011).
7. Weiner, S., Levi-Kalisman, Y., Raz, S. & Addadi, L. "Biologically Formed Amorphous Calcium Carbonate." *Connect. Tissue Res.* **44,** 214–218 (2003).
8. Politi, Y. "Sea Urchin Spine Calcite Forms via a Transient Amorphous Calcium Carbonate Phase." *Science* **306,** 1161–1164 (2004).
9. Demichelis, R., Raiteri, P., Gale, J. D. & Dovesi, R. "The multiple structures of vaterite." *Cryst. Growth Des.* **13,** 2247–2251 (2013).
10. Bryce, D. L., Bultz, E. B. & Aebi, D. "Calcium-43 Chemical Shift Tensors as Probes of Calcium Binding Environments. Insight into the Structure of the Vaterite CaCO3 Polymorph by 43Ca Solid-State NMR Spectroscopy." *J. Am. Chem. Soc.* **130,** 9282–9292 (2008).
11. Kabalah-Amitai, L., Mayzel, B., Kauffmann, Y., Fitch, A. N., Bloch, L., Gilbert, P. U. P. A. & Pokroy, B. "Vaterite Crystals Contain Two Interspersed Crystal Structures." *Science* **340,** 454–457 (2013).

12. Beaudoin, J. J., Gu, P. & Lin, W. "Flexural Behavior of Cement Systems Reinforced with High Aspect Ratio Aragonite Micro-Fibres." *Cem. Concr. Res.* **26,** 1775–1777 (1996).
13. Park, W. K., Ko, S. J., Lee, S. W., Cho, K. H., Ahn, J. W. & Han, C. "Effects of magnesium chloride and organic additives on the synthesis of aragonite precipitated calcium carbonate." *J. Cryst. Growth* **310,** 2593–2601 (2008).
14. Forsgren, J., Andersson, M., Nilsson, P. & Mihranyan, A. "Mesoporous Calcium Carbonate as a Phase Stabilizer of Amorphous Celecoxib – An Approach to Increase the Bioavailability of Poorly Soluble Pharmaceutical Substances." *Adv. Healthc. Mater.* **2,** 1469–1476 (2013).
15. Mori, Y., Enomae, T. & Isogai, A. "Application of Vaterite-Type Calcium Carbonate Prepared by Ultrasound for Ink Jet Paper." *J. Imaging Sci. Technol.* **54,** 1–6 (2010).
16. Tewes, F., Gobbo, O. L., Ehrhardt, C. & Healy, A. M. "Amorphous Calcium Carbonate Based-Microparticles for Peptide Pulmonary Delivery." *Appl. Mater. Interfaces* **8,** 1164–1175 (2016).
17. Kim, Y. Y., Hetherington, N. B. J., Noel, E. H., Kröger, R., Charnock, J. M., Christenson, H. K. & Meldrum, F. C. "Capillarity creates single-crystal calcite nanowires from amorphous calcium carbonate." *Angew. Chemie - Int. Ed.* **50,** 12572–12577 (2011).
18. Li, X., Chang, W. C., Chao, Y. J., Wang, R. & Chang, M. "Nanoscale structural and mechanical characterization of a natural nanocomposite material: The shell of red abalone." *Nano Lett.* **4,** 613–617 (2004).
19. Reeder, R. J., Tang, Y., Schmidt, M. P., Kubista, L. M., Cowan, D. F. & Phillips, B. L. "Characterization of Structure in Biogenic Amorphous Calcium Carbonate: Pair Distribution Function and Nuclear Magnetic Resonance Studies of Lobster Gastrolith." *Cryst. Growth Des.* **13,** 1905–1914 (2013).
20. Weller, M., Overton, T., Rourke, J. & Armstrong, F. "*Inorganic Chemistry*." (Oxford University Press).

21. Xiao, J. & Yang, S. "Polymorphic and morphological selection of CaCO3 by magnesium-assisted mineralization in gelatin: magnesium-rich spheres consisting of centrally aligned calcite nanorods and their good mechanical properties." *CrystEngComm* **13,** 2472 (2011).
22. Hu, Z., Shao, M., Li, H., Cai, Q., Zhong, C., Xianming, Z. & Deng, Y. "Synthesis of Needle-Like Aragonite Crystals in the Presence of Magnesium Chloride and Their Application in Papermaking." *Adv. Compos. Mater.* **18,** 315–326 (2009).
23. Andreassen, J.-P., Beck, R. & Nergaard, M. "Biomimetic type morphologies of calcium carbonate grown in absence of additives." *Faraday Discuss.* **159,** 247 (2012).
24. Navrotsky, A. "Energetic clues to pathways to biomineralization: precursors, clusters, and nanoparticles." *Proc. Natl. Acad. Sci. U. S. A.* **101,** 12096–12101 (2004).
25. Radha, A. V, Forbes, T. Z., Killian, C. E., Gilbert, P. U. P. A. & Navrotsky, A. "Transformation and crystallization energetics of synthetic and biogenic amorphous calcium carbonate." *Proc. Natl. Acad. Sci. U. S. A.* **107,** 16438–16443 (2010).
26. Kawano, J., Shimobayashi, N., Miyake, A. & Kitamura, M. "Precipitation diagram of calcium carbonate polymorphs: its construction and significance." *J. Phys. Condens. Matter* **21,** 1–6 (2009).
27. Politi, Y., Batchelor, D. R., Zaslansky, P., Chmelka, B. F., Weaver, J. C., Sagi, I., Weiner, S. & Addadi, L. "Role of Magnesium Ion in the Stabilization of Biogenic Amorphous Calcium Carbonate : A Structure - Function Investigation." *Chem. Mater.* **22,** 161–166 (2010).
28. Gal, A., Weiner, S. & Addadi, L. "The Stabilizing Effect of Silicate on Biogenic and Synthetic Amorphous Calcium Carbonate." *J. Am. Chem. Soc.* **132,** 13208–13211 (2010).
29. Berman, A., Addadi, L., Kvick, A., Leiserowitz, L., Nelson, M. & Weiner, S. "Intercalation of sea urchin proteins in calcite: study of a crystalline composite material." *Science* **250,** 664–667 (1990).
30. Addadi, B. L., Raz, S. & Weiner, S. "Taking Advantage of Disorder : Amorphous Calcium Carbonate and Its Roles in Biomineralization." *Adv. Mater.* **15,** 959–970 (2003).

31. Aizenberg, J., Lambert, G., Weiner, S. & Addadi, L. "Factors involved in the formation of amorphous and crystalline calcium carbonate: a study of an ascidian skeleton." *J. Am. Chem. Soc.* **124,** 32–39 (2002).
32. Smith, B. J., Rawal, A., Funkhouser, G. P., Roberts, L. R., Gupta, V., Israelachvili, J. N. & Chmelka, B. F. "Origins of saccharide-dependent hydration at aluminate, silicate, and aluminosilicate surfaces." *Proc. Natl. Acad. Sci.* **108,** 8949–8954 (2011).
33. Meiron, O. & Ashkenazi, B. "Method for producing stabilized amorphous calcium carbonate." (2014).
34. Nebel, H., Neumann, M., Mayer, C. & Epple, M. "On the structure of amorphous calcium carbonate--a detailed study by solid-state NMR spectroscopy." *Inorg. Chem.* **47,** 7874–7879 (2008).
35. Bryce, D. L. "Calcium binding environments probed by 43Ca NMR spectroscopy." *Dalt. Trans.* **39,** 8593–8602 (2010).
36. "*Applications of Ion Chromatography for Pharmaceutical and Biological Products*." (John Wiley & Sons, Inc., 2012). doi:10.1002/9781118147009
37. Larson, D. J., Middle, L., Vu, H., Zhang, W., Serianni, A. S., Duman, J. & Barnes, B. M. "Wood frog adaptations to overwintering in Alaska: new limits to freezing tolerance." *J. Exp. Biol.* **217,** 2193–2200 (2014).
38. Hubalek, Z. "Protectants used in the cryopreservation of microorganisms." *Cryobiology* **46,** 205–229 (2003).
39. Smith, B. J., Roberts, L. R., Funkhouser, G. P., Gupta, V. & Chmelka, B. F. "Reactions and Surface Interactions of Saccharides in Cement Slurries." *Langmuir* **28,** 14202–14217 (2012).
40. Wang, S. S. & Xu, A. W. "Amorphous calcium carbonate stabilized by a flexible biomimetic polymer inspired by marine mussels." *Cryst. Growth Des.* **13,** 1937–1942 (2013).
41. Maier, G. P., Rapp, M. V., Waite, J. H., Israelachvili, J. N. & Butler, A. "Adaptive Synergy Between Catechol and Lysine Promotes Wet Adhesion by Surface Salt Displacement." *Science* **349,** 628–631 (2015).
42. Zhang, Z., Xie, Y., Xu, X., Pan, H. & Tang, R. "Transformation of amorphous calcium carbonate into aragonite." *J. Cryst. Growth* **343,** 62–67 (2012).

6. Appendices

6.1. Crystallization and aggregation during TEM imaging

Significant issues were encountered while performing transmission electron microscopy on the amorphous calcium carbonate nanoparticles. As amorphous calcium carbonate is a soft matter which is quickly crystallized by both pressure and heat, it was not surprising that the electron beam induced both particle aggregation and crystallization. Although lower electron beam voltages were used and cryogenic TEM was performed on the material, neither the reduction in voltage nor the reduction in temperature mediated the aggregation and crystallization processes to a large extent. Changing the quantity of electrons (current) that passed through the sample by adjusting the spot size did, however, significantly affect the process. At low spot sizes (higher current), particle aggregation was not able to be imaged as it occurred instantaneously and crystallites were immediately visible (Figure 23). The darker spots (1-2 nm) in the bright field image collected at spot size 2 signify areas of higher density. These correspond with the crystalline regions in the sample as the crystallites scatter electrons to a larger extent than the less dense, lighter amorphous material. The selected area electron diffraction pattern confirms that crystallites were present in the material, as the electron diffraction rings are composed of distinct spots. Increasing the spot size to 5 slowed particle agglomeration to an extent that it was able to be imaged (Figure 24). The bright field images collected over a series of three minutes show the particles fusing together under the electron beam, although no crystallites were formed during this time as particle aggregation occurs more quickly than crystallization. Increasing the spot size to 7 allowed for adequate imaging of the particles without extensive agglomeration; the distinct features of the particles are visible in the bright field images for 5-10 minutes with limited fusion (Figure 25). These

conditions (spot size 7, 300 kV) were used to obtain the TEM images shown in Figures 9, 10, 16, and 20.

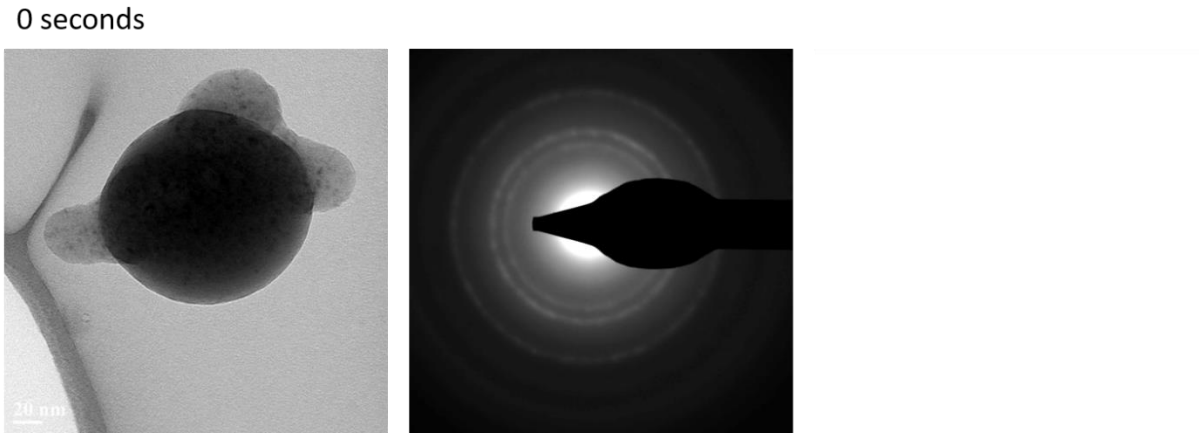

Figure 23. Bright-field transmission electron micrograph and corresponding selected area electron diffraction pattern acquired for neat amorphous calcium carbonate under a 300 kV electron beam with a spot size of 2.

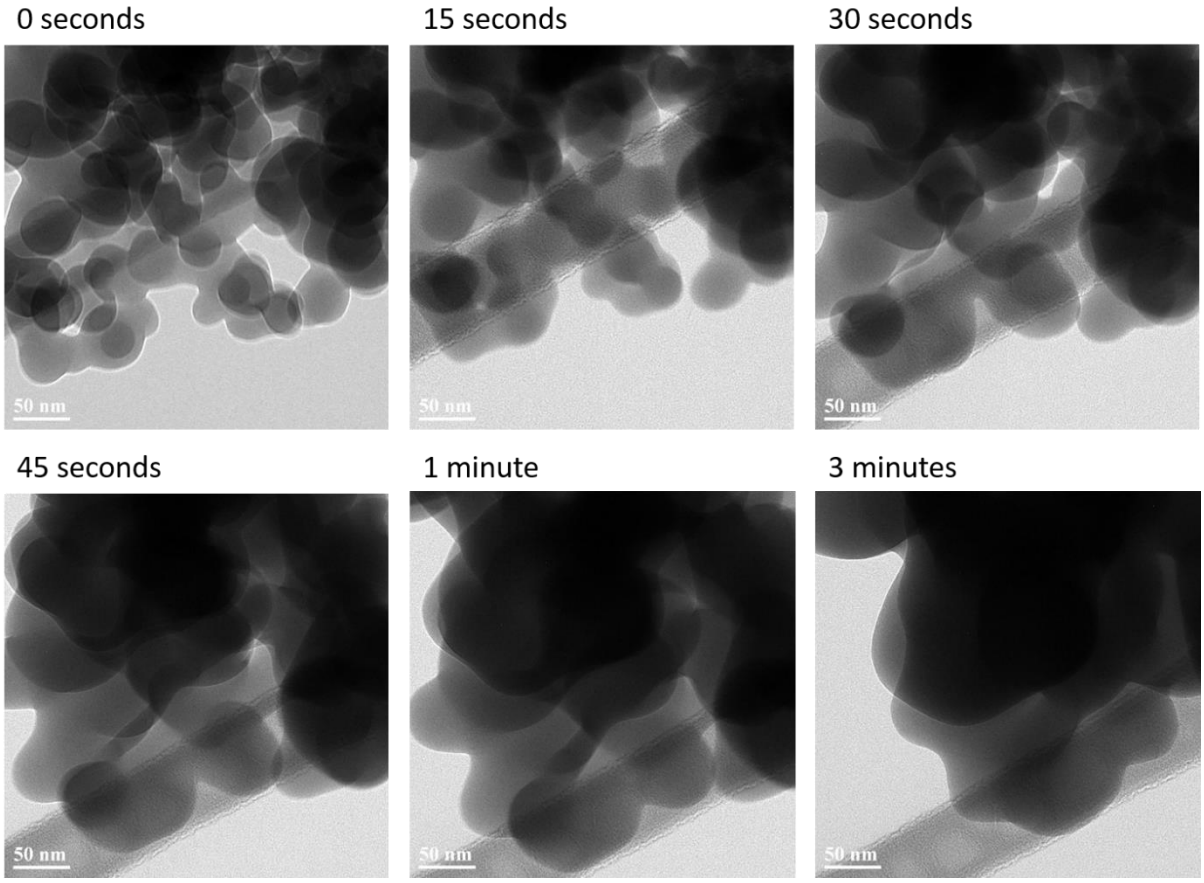

Figure 24. Bright-field transmission electron micrographs acquired as a function of time for neat amorphous calcium carbonate under a 300 kV electron beam with a spot size of 5.

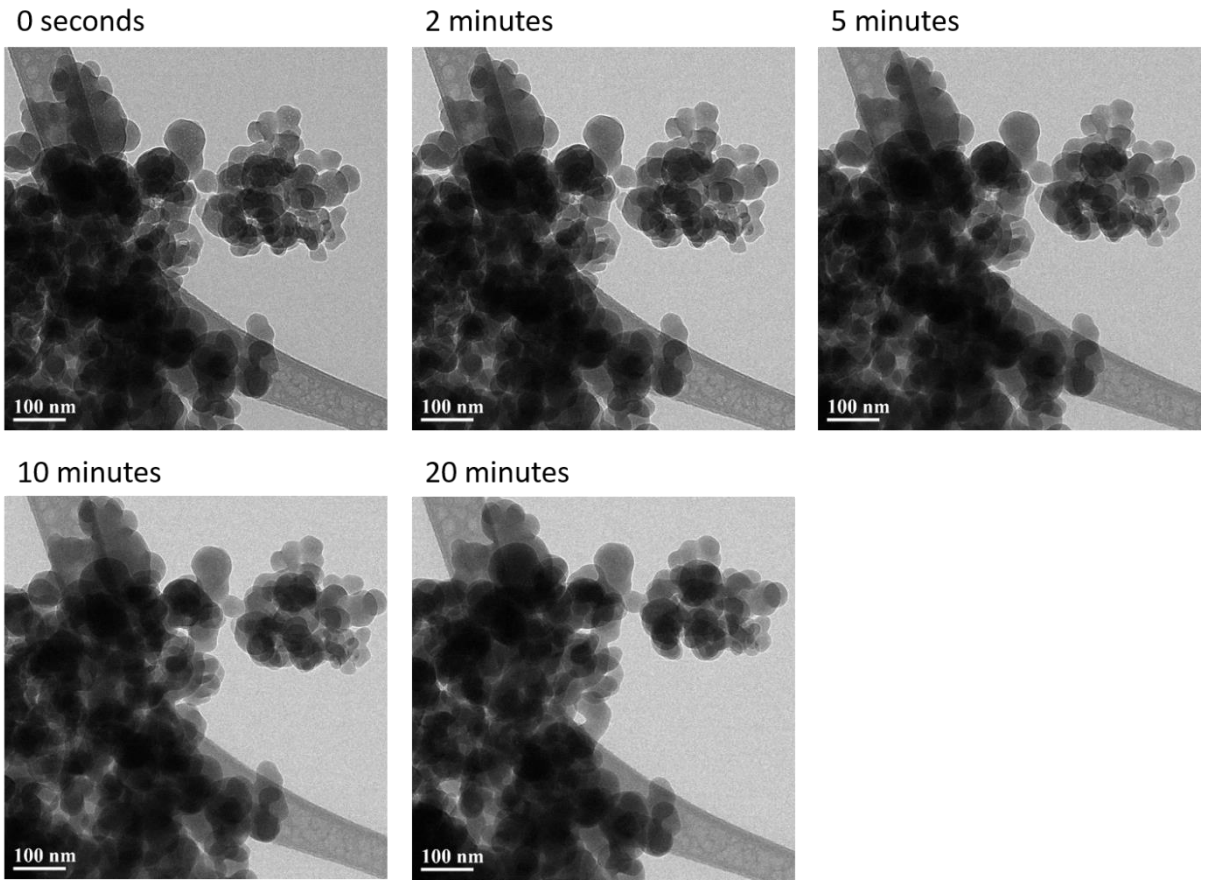

Figure 25. Bright-field transmission electron micrographs acquired as a function of time for neat amorphous calcium carbonate under a 300 kV electron beam with a spot size of 7.

6.2. Crystallization during NMR measurements

As the metastable nature of the amorphous calcium carbonate was highlighted in the previous section, it was again unsurprising when the material crystallized while NMR measurements were being obtained. The fully amorphous sample (Figure 26, Pre-NMR) was packed into a rotor and spun at 10 kHz for three hours while measurements were collected. An XRD pattern was obtained after these measurements for both the sample in the rotor (Figure 26, Post-NMR) and the sample that remained stored at 76% relative humidity for 3 hours (Figure 26, Control). Calcite and vaterite reflections are present in the pattern acquired for the material that was spun in the rotor, but not in the pattern acquired for the control. There are two potential explanations for this phenomenon; the first is that the temperature of

the rotor and material increased as a result of the friction at high spinning speeds and the heat induced crystallization and the second is that the centrifugal force exerted a significant pressure on the material at 10 kHz and induced crystallization. Both heat and pressure are known to induce crystallization in amorphous calcium carbonate. As a result of these observations, all NMR measurements in this thesis were performed on fully ^{13}C enriched samples to reduce the number of scans necessary for adequate signal and therefore reduce the amount of time that the material spent spinning in the spectrometer (3 hours was reduced down to 5 minutes). The alternative solution not tested was to reduce the temperature of the sample and rotor in the probe using liquid nitrogen cooling.

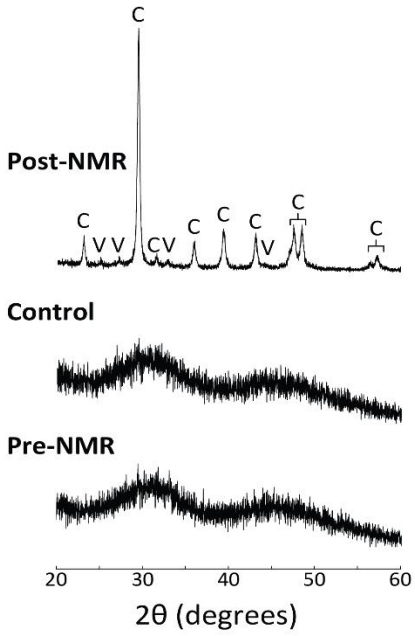

Figure 26. Wide-angle XRD patterns acquired for neat calcium carbonate before NMR measurements were performed (pre-NMR), after three additional hours of storage at 76% relative humidity (control), and after three hours of NMR measurements were conducted (post-NMR).